Nonequilibrium Potential in Reaction-Diffusion Systems

Horacio S. Wio[1,2]

[1] Centro Atómico Bariloche, CNEA, and Instituto Balseiro, UNC, 8400-San Carlos de Bariloche, Argentina
[2] Consejo Nacional de Investigaciones Científicas y Técnicas, Argentina
wio@cab.cnea.gov.ar

Summary. In this set of lectures I present a brief review of the general issue of pattern formation in reaction-diffusion systems emphasizing the point of view of the concept of the nonequilibrium potential. Through some simple examples I discuss the possibilities of exploiting this concept in order to describe the decay of metastable states and introduce an analysis of the stochastic resonance phenomenon in extended systems .

1 Introduction

The subject of pattern formation far from equilibrium has captured the attention of researchers for more than a decade, and is by now one of the most active fields in the physics of complex systems. ([63, 23, 68, 15, 44, 51, 60, 45, 7, 78, 58, 61, 53, 52, 41, 54, 8, 82, 62]) The extremely rich variety of nonequilibrium systems that one can consider calls for different descriptions. Among them, the reaction-diffusion (RD) approach has shown to be a very fertile source of models for interesting phenomena in the natural and social sciences, where structures can arise and last for longer or shorter periods of time according to their degree of stability. ([63, 23, 68, 15, 44, 51, 78, 58, 53, 8, 82])

From the equilibrium phenomena point of view, both classical mechanics and reversible equilibrium thermodynamics (the two most prominent branches of macroscopic physics) are characterized by **extremum principles**. In classical mechanics it is the principle of stationary action that determines the classical trajectory, while equilibrium thermodynamics is characterized by the maximum entropy principle in closed systems. Both extremum principles originate as the macroscopic limit of more fundamental theories (quantum mechanics and statistical mechanics respectively) where those principles are violated through the occurrence of fluctuations: quantum fluctuations on one hand (that assign finite probability amplitudes to nonclassical trajectories) and thermal fluctuations (assigning nonzero probabilities to states with less than the maximum entropy) on the other. It is this deep connection between fluctuation phenomena and extremum principles that allows the system to explore a neighborhood of the extremizing state and thereby identify the extremum.

The evolution equations governing the nonequilibrium phenomena belong neither to the realm of equilibrium thermodynamics (therefore thermodynamic extremum principles are not applicable) nor to the realm of classical mechanics (implying that the principle of least action is also not applicable). Hence, an extremum principle allowing to characterize time-dependent or time-independent solutions of such evolution equations is not readily available. However, classical fluctuations are also present in nonequilibrium systems, just from thermal origin or due to some stochastic perturbations of general nature. Just as in equilibrium thermodynamics, these fluctuations allow to explore not only the deterministic nonequilibrium trajectory, but also its neighborhood. Hence, it is expected that some extremum principle must also hold when one is able to identify the minimized potential function, enabling us to characterize stable steady states (or attractors) of the macroscopic evolution equations (as well as the unstable ones or separatrices) by some extremum condition. This is what one seeks in order to understand pattern selection in self-organizing systems and other related phenomena.

The main goal of these lectures is offering an introductory view to the application of the nonequilibrium potential picture into reaction-diffusion systems. We can summarize the main idea behind the nonequilibrium potential approach by saying that the selection of a pattern is strongly influenced by fluctuations. It is only *chance* that could decide through the effect of *fluctuations.* The fluctuations will enable us to explore the **landscape** of the system, and after making some initial unsuccessful attempts finally a particular fluctuation will take over. It is within this framework that the interplay between chance and constraint, or fluctuations and irreversibility, underlying all instability phenomena, is clearly seen. ([63, 23, 68, 51, 61, 53, 82, 62])

In the next sections we will review a few concepts on dynamical systems, on stochastic processes and on reaction-diffusion systems as well. Afterwards, we will show a few simple cases where the nonequilibrium potential in reaction-diffusion systems can be evaluated. In the final sections we will show applications of these nonequilibrium potentials in order to analyze the probability of decay of extended metastable states as well as the phenomenon of stochastic resonance in extended systems.

2 Dynamical Systems: Stability

Physics courses have taught us that the evolution of the state variables of a system (for instance, obeying the laws of classical physics) is given by a set of differential equations of first order in time. These may be ordinary differential equations (ode) -like Hamilton's equations or the chemical kinetic equations in a well stirred reactor-; or partial differential equations (pde) -like the fluid dynamics equations or the nonlinear reaction-diffusion equations-. In the latter case, i.e. pde, which are typical in macroscopic descriptions, one deals with an infinite number of degrees of freedom, corresponding to the

values of the state variables or "fields" (for instance, reactant concentrations, order parameters, etc) at each space point as functions of time.

Although in many problems this aspect may constitute the essential characteristic of the phenomenon under study, it is not unusual that the description can be reduced to a finite number of variables. The study of systems with a finite number of variables, that is of ode's, will give us the chance to learn a few more or less standard techniques to analyze not only systems of ode's but that are also adequate to deal with some problems describable by pde's.

Hence we will start considering a set of ode's assuming that the constraints acting on the system do not depend explicitly on time (i.e. an *autonomous* system), that will have the general form ([63, 60, 7, 61, 8, 82, 62])

$$\frac{\mathrm{d}\boldsymbol{x}}{\mathrm{d}t} = \boldsymbol{F}(\boldsymbol{x}, \zeta) \tag{1}$$

with $\boldsymbol{x} = (x_1, x_2, ..., x_n)$ and $\boldsymbol{F}(\boldsymbol{x}, \zeta) = (F_1(\boldsymbol{x}, \zeta), F_2(\boldsymbol{x}, \zeta), ..., F_n(\boldsymbol{x}, \zeta))$. Here x_j correspond to the state variables while ζ are some parameters (that we will denote hereafter as *control parameters*) corresponding to the systems' internal structure (diffusion coefficients, viscosities, etc) or to the form of relating with external world (thermal or shear constraints, densities of chemicals pumped in or out of a reactor). The $F_j(\boldsymbol{x}, \zeta)$ are in general nonlinear functions of the x_j, this nonlinearity being the characteristic that does not allow us to derive explicit solutions for these systems using standard methods.

The evolution of the system described by (1) is embedded in a n-dimensional space spanned by the full set of variables $\boldsymbol{x} = (x_1, x_2, ..., x_n)$ which we call the *phase space* Γ. The instantaneous state of the system is given by a particular set of values $(x_1, x_2, ..., x_n)$ or a unique point $\boldsymbol{P}$ in phase space. That means a one-to-one correspondence between the system physical states and the phase points.

A succession of states $(\boldsymbol{x}, ..., \boldsymbol{x}_t, ...)$, attained along the course of time t, will determine a succession of points $(\boldsymbol{P}, ..., \boldsymbol{P}_t, ...)$ in phase space joined by a curve C, corresponding to a phase trajectory. Repeating the process for all possible sets $(\boldsymbol{x'}, ..., \boldsymbol{x'}_t, ...)$ one generates a continuous family of phase space trajectories indicating that the evolution of the system corresponds to a mapping of Γ into itself.

The set of points $\boldsymbol{x}_s$ where

$$F_1(\boldsymbol{x}_s, \zeta) = F_2(\boldsymbol{x}_s, \zeta) = ... = F_n(\boldsymbol{x}_s, \zeta) = 0, \tag{2}$$

(correspondingly $\dot{x}_1 = \dot{x}_2 = ... = \dot{x}_n = 0$) are called *singular* or *fixed points* (in autonomous systems singular points remain fixed in phase space). Fixed points correspond to *stationary states* that can eventually be reached after the evolution of the system. The objects embedded in the phase space that are bounded and are mapped into themselves during the evolution generated by (1) are called *invariant manifolds*. For instance, fixed points are invariant

manifolds of dimension $d = 0$. The importance of these invariant manifolds arises from the fact that they offer a geometrical view of the dynamical system.

At this point it is worth refereing to the conservative or dissipative character of the system under study. Let us consider the probability density $f(x_1, x_2, ..., x_n, t)$ ([69, 43, 39, 82]) that, after multiplying by $\mathrm{d}x_1\mathrm{d}x_2...\mathrm{d}x_n$, gives the probability of finding the system in the neighborhood of the phase space point $(x_1, x_2, ..., x_n)$. The Liouville or evolution equation for this density is ([69, 43, 39, 82])

$$\frac{\partial f}{\partial t} + \sum \frac{\partial}{\partial x_i}(f F_i) = 0 \tag{3}$$

that can be rewritten as

$$\frac{\mathrm{d} \ln f}{\mathrm{d}t} = -\nabla \boldsymbol{F}. \tag{4}$$

We will hence define that a system is conservative if

$$\nabla \boldsymbol{F} = 0$$

as for a harmonic oscillator; while we define a dissipative system according to

$$\overline{\nabla \boldsymbol{F}} < 0$$

(where we used the average $\overline{\nabla \boldsymbol{F}} = T^{-1} \int_0^T \nabla \boldsymbol{F} \mathrm{d}t'$), as for instance, in a damped harmonic oscillator. It is clear that a conservative system will conserve (but perhaps deform) the initial volume $\Delta\Gamma_0$ in phase space. On the other hand, a dissipative system will be such that $\Delta\Gamma_0 \to \Delta\Gamma_f$ for $t \to \infty$, where $\Delta\Gamma_f$ is a subset with a lower dimension than the phase space (and with zero volume). Hence, it is in this last case that the system can evolve towards a fixed point that, in this case, is called an *attractor*. ([63, 23, 76, 61, 53, 82])

The relevant question here concerns the stability of the indicated solutions (or invariant manifolds) of the system of nonlinear differential equations (NLDE), that is what happens when such a solution is perturbed: does the system return to the fixed point or move away from it?.

2.1 Linear Stability: Two Variable Systems

In order to introduce some basic notions of *linear stability theory*, we will restrict ourselves to a set of two first order NLDE, corresponding to a general second order autonomous system, i.e. :

$$\begin{aligned} \frac{\mathrm{d}x_1}{\mathrm{d}t} &= F_1(x_1, x_2) \\ \frac{\mathrm{d}x_2}{\mathrm{d}t} &= F_2(x_1, x_2) \end{aligned} \tag{5}$$

If, for certain values of the coordinates, say (x_1^0, x_2^0), the functions F_1 and F_2 satisfy very general (Lipschitz) conditions ([62]), equations (5) have a unique solution in the neighborhood of the point (x_1^0, x_2^0). In what follows, we shall assume that these conditions are satisfied.

Through any point (x_1^0, x_2^0) there is a unique phase curve, with the exception of the *singular* or *fixed points* (x_1^s, x_2^s), where $\dot{x}_1 = \dot{x}_2 = 0$. A fixed point, corresponding to a steady state solution of (5), can always be moved to the origin by the change of variables $x_1 \to x_1 - x_1^s$ and $x_2 \to x_2 - x_2^s$. Therefore, we shall assume that the singular point is located at the origin. We then consider a system described by (5) which is in a steady state at $(x_1^s, x_2^s) = (0, 0)$.

If the system is in the steady state, it is important to know how it will behave under the influence of a small perturbation. Here we face several possibilities. The system can leave this steady state and move to another one; it can remain in the neighborhood of the original steady state; or it can decay back to the original state. In order to analyze the different possibilities we use a *linear stability analysis*. ([63, 23, 14, 7, 82, 62]) By this procedure we can say something regarding the stability of the system in the neighborhood of the steady state, but nothing about the global stability of the system. To discuss stability in the neighborhood of the steady state we write the solution in terms of the departure from the steady state, i.e. :

$$x_1 = x_1^s + \delta x_1; \quad x_2 = x_2^s + \delta x_2 \tag{6}$$

inserting this into (5), using $x_1^s = x_2^s = 0$, and expanding up to first order in the departures $(\delta x_1, \delta x_2)$ we obtain:

$$\begin{aligned} \dot{x}_1 &= \delta\dot{x}_1 = F_1(0,0) + \left(\frac{\partial F_1}{\partial x_1}\right)_0 \delta x_1 + \left(\frac{\partial F_1}{\partial x_2}\right)_0 \delta x_2 + O(\delta x_1^2, \delta x_2^2) \\ \dot{x}_2 &= \delta\dot{x}_1 = F_2(0,0) + \left(\frac{\partial F_2}{\partial x_1}\right)_0 \delta x_1 + \left(\frac{\partial F_2}{\partial x_2}\right)_0 \delta x_2 + O(\delta x_1^2, \delta x_2^2) \end{aligned} \tag{7}$$

Keeping in mind that $F_1(0,0) = F_2(0,0) = 0$, calling

$$\left(\frac{\partial F_1}{\partial x_1}\right)_0 = a; \quad \left(\frac{\partial F_1}{\partial x_2}\right)_0 = b; \quad \left(\frac{\partial F_2}{\partial x_1}\right)_0 = c; \quad \left(\frac{\partial F_2}{\partial x_2}\right)_0 = d,$$

and considering very small values of the δx_j, so that we can neglect higher order terms, we reduce the problem to the analysis of the following linear system

$$\begin{pmatrix} \delta\dot{x}_1 \\ \delta\dot{x}_2 \end{pmatrix} = \begin{bmatrix} a & b \\ c & d \end{bmatrix} \begin{pmatrix} \delta x_1 \\ \delta x_2 \end{pmatrix} = \mathbb{M} \begin{pmatrix} \delta x_1 \\ \delta x_2 \end{pmatrix} \tag{8}$$

The solutions of (8) give the parametric forms of the phase curves in the neighborhood of the steady state (at the origin), with time as the parameter.

The general form of the solution of (8) (except when $\lambda_1 = \lambda_2$) is

$$\begin{pmatrix} \delta x_1 \\ \delta x_2 \end{pmatrix} = \alpha \hat{c}_1 \mathrm{e}^{-\lambda_1 t} + \beta \hat{c}_2 \mathrm{e}^{-\lambda_2 t} \tag{9}$$

where α and β are arbitrary constants, $\hat{c}_1$ and $\hat{c}_2$ are the eigenvectors (the *normal modes*) of the matrix $\mathbb{M}$, associated to the eigenvalues λ_1 and λ_2 respectively. These eigenvalues are determined from the relation

$$\det(\mathbb{M} - \lambda \mathbb{1}) = 0$$

yielding

$$\lambda_{1,2} \;=\; \frac{1}{2}(a+d) \pm [(a+d)^2 - 4(ad-bc)]^{1/2}$$

It is thus clear that the temporal behavior of the system, originally in the steady state $(x_1^s, x_2^s) \;=\; (0,0)$, after applying a small perturbation, will depend on the characteristics of the eigenvalues λ_j. We have the following possibilities:
(i) Both eigenvalues, λ_1 and λ_2, are real and negative ($\lambda_1 \;<\; \lambda_2 \;<\; 0$);
(ii) both eigenvalues are real and positive ($0 \;<\; \lambda_1 \;<\; \lambda_2$);
(iii) both eigenvalues are real, but $\lambda_1 \;<\; 0 \;<\; \lambda_2$;
(iv) both eigenvalues are pure imaginary;
(v) both eigenvalues are complex conjugates with $\mathcal{R}e(\lambda_1) \;=\; \mathcal{R}e(\lambda_2) \;<\; 0$;
(vi) both eigenvalues are complex conjugates with $\mathcal{R}e(\lambda_1) \;=\; \mathcal{R}e(\lambda_2) \;>\; 0$.

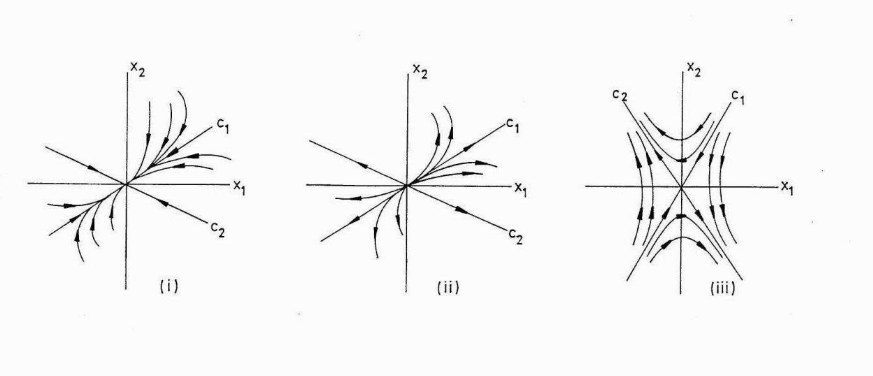

Fig. 1. The phase portrait for the different types of fixed points.

Some of the situations that could arise, according to the kind of eigenvalues we find, correspond to the phase trajectories depicted in Fig. 1. Case (i) corresponds to a solution that decays for increasing time, and is called a *stable node*. Case (ii) is the opposite situation, and corresponds to an *unstable node*. Case (iii) is intermediate between the two previous situations: it is stable in one direction and unstable in the other, this corresponds to a *saddle point*. Not shown are the cases corresponding to periodic behavior: with a

constant amplitude or *center*, with a decaying amplitude, or *stable focus*, and its opposite or *unstable focus*.

Within this general scheme, even when we extend the results to a larger number of variables, it is possible to identify three basic situations: (a) $\mathcal{R}e(\lambda_j) < 0$ for all j; (b) at least one $\mathcal{R}e(\lambda_j) > 0$; (c) at least one $\mathcal{R}e(\lambda_j) = 0$. The above analysis yields the following results (remember that all this corresponds to *small perturbations*!) :
(a) All $\mathcal{R}e(\lambda_j) < 0$: the steady state is called *asymptotically stable*. Whatever the form of the nonlinear terms in Eq.(3), after a small perturbation the normal modes decay to it. These types of solution are called *attractors*, and the region of phase space including all the points such that any initial state finally tends to the attractor form its *basin of attraction*.
(b) At least one $\mathcal{R}e(\lambda_j) > 0$: the steady state is *unstable*, that is, the normal mode associated with this eigenvalue will grow with time.
In either case (a) or (b), the behavior of the individual modes will be oscillatory if $\mathcal{I}m(\lambda_j) \neq 0$, and monotonic otherwise.
(c) At least one $\mathcal{R}e(\lambda_j) = 0$, all other $\mathcal{R}e(\lambda_k) < 0$: the steady state is *marginally stable* with respect to the mode having $\mathcal{R}e(\lambda_j) = 0$. As a solution of the linearized equation this mode will neither grow nor decay, but could oscillate if in addition it has $\mathcal{I}m(\lambda_j) \neq 0$. Here, the explicit form of the nonlinear terms will determine whether this marginally stable steady state is stable or unstable.

For the case when several fixed points coexist, the basin of attraction of each attractor is separated from the others by curves of *neutral* points, known as *separatrices*.

Besides the cases we have just analyzed, for nonconservative nonlinear equations it is also possible to find another, very important, kind of steady solution, called *limit cycle*, corresponding to stable (and also unstable) *periodic* solutions. If such a periodic solution is stable, all the solutions in its neighborhood will decay to it for long times. We show a typical phase portrait in Fig. 2.

To exemplify this behavior consider the system

$$\dot{x} = \ y + x[1-\rho]\rho^{-1/2}$$

$$\dot{y} = -x + y[1-\rho]\rho^{-1/2}$$

with $\rho = x^2 + y^2$. It is left to the reader to prove that this system has a limit cycle attractor (hint: use polar coordinates).

2.2 Bifurcations

According to the above classification one might be tempted to conclude that a given system can only be described by a particular kind of fixed point or attractor. But this is not the case. The most interesting aspects of nonequilibrium phenomena arise from the fact that the same system can show a

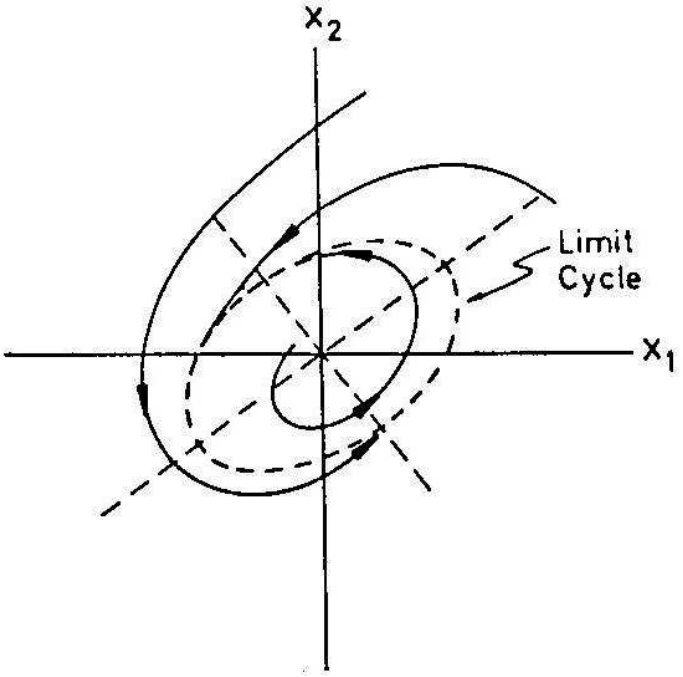

Fig. 2. The phase portrait for a limit cycle.

variety of behaviors, each one corresponding to a different attractor. The change from a given state to another is produced by the variation of some of the external constraints (or external parameters) acting on the system, so that the original (or *reference*) state becomes unstable, and subsequently a *bifurcation* to new branches of states occurs. ([63, 23, 82, 62])

We will analyze two kinds of instabilities which may lead to a stable limit cycle from a fixed point. For our discussion we will refer to Fig. 3. In part (i) of the figure we depict the variation of the eigenvalue λ associated with the unstable original mode. This is usually called *the thermodynamic branch* as it is the direct extrapolation of the equilibrium states, sharing with them the property of asymptotic stability, since in this range the system is able to damp internal fluctuations or external disturbances, and we can still describe the behavior of the system, essentially, within a thermodynamic approach. The horizontal axis indicates the real part of the eigenvalue and the vertical axis the imaginary part. The real part of λ crosses the imaginary axis, from the negative to the positive values (left to right), as the control parameter ζ takes a critical value $\zeta = \zeta_c$. In part (ii) and (iii) of the figure, the horizontal axis represents the variation of the control parameter ζ, and the vertical axis schematically indicates a steady state solution of the NLDE describing the system and may represent several different physical or chemical properties

(e.g. a concentration of some reactive for a chemical system, an amplitude of oscillation for a mode in a fluid, etc).

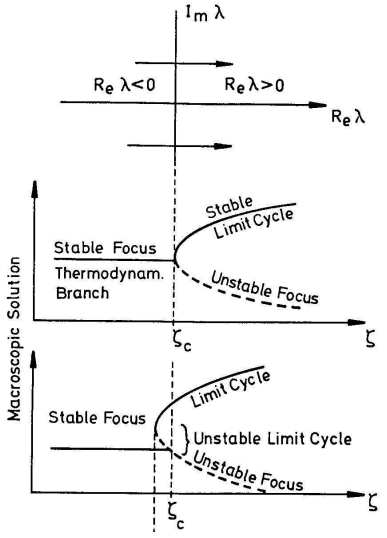

Fig. 3. Schematic picture of the bifurcation process.

As the parameter ζ is varied from left to right (in parts (ii) and (iii) of the figure), a pair of complex eigenvalues λ crosses the imaginary axis (part (i)). Consider the case where, before crossing, the steady state solution (x_1^0, x_2^0) is a *stable focus*. As soon as $\mathcal{R}e(\lambda)$ goes through zero and becomes positive for $\zeta = \zeta_c$, the solution may :
(a) Bifurcate into an unstable *focus* and a stable *limit cycle*. Beyond the bifurcation point ζ_c, the limit cycle is the only stable solution. This kind of transition, where the limit cycle arises continuously for $\zeta > \zeta_c$, is called a *soft self-excitation*. A bifurcation to the right is called a *supercritical* one.
(b) The bifurcation to a limit cycle may also be subcritical, that is, it may occur to the left of $\zeta = \zeta_c$ as indicated in part (iii). The limit cycle towards which the system bifurcates at ζ_c is unstable, and a stable limit cycle may be reached for $\zeta_a < \zeta < \zeta_c$ but only in response to a finite perturbation that exceeds a certain threshold. For a smaller perturbation, the system will return to the stable steady state. But if the perturbation exceeds the threshold (as indicated in the figure) then it will continue to grow until the system reaches a stable limit cycle. Due to the existence of a threshold this is called a *hard self-excitation*. For small perturbations the system will remain in the stable steady state until $\zeta > \zeta_c$, where the steady state becomes unstable and the system jumps *abruptly* to the limit cycle, in contrast to the *continuous* transition of

the previous case. Mathematically both types of instabilities are classified as *Hopf's bifurcations*. ([63, 58, 62])

When discussing the kind of transitions associated with nonequilibrium instabilities, it is usual to adopt the language of equilibrium thermodynamic phase transitions and critical phenomena. For instance, the supercritical bifurcation is analogous to a second-order phase transition, while the subcritical resembles a first-order one.

2.3 Kinetic Potential, Symmetry Breaking

Now, and in order to introduce some notions related to the concept of *symmetry breaking* as well as with *global stability*, we will work out a useful mechanical analogy. Let us analyze the example of a *damped nonharmonic oscillator*. ([23, 68]) The classical equation of motion of such a system is

$$m\,\frac{\mathrm{d}v}{\mathrm{d}t} \;=\; -\;\gamma v \;+\; F(x), \tag{10}$$

where x is the position and v is the velocity of a particle of mass m, γ is the friction coefficient and $F(x)$ an external force. Considering that $v = \mathrm{d}x/\mathrm{d}t$, (10) can be rewritten as

$$m\ddot{x} + \gamma\dot{x} = F(x). \tag{11}$$

We will concentrate on the particular case in which the particle is light (its mass m is very small) while the friction coefficient (γ) is very large. This corresponds to *overdamped motion*, in which the first term on the left hand side, when compared to the second, can be neglected (that is: we assume $\ddot{x} \approx 0$), in what is a prototype of *adiabatic elimination procedures*. ([23, 76, 17]) Now we can make a change of time scale according to $t \to \gamma t$, and in this way eliminate the constant γ from the equation, which finally reads

$$\dot{x} \;=\; F(x). \tag{12}$$

It has the same form as the equation we have analyzed before (i.e. Eq.(1)). Now, for a one dimensional problem, we have that the force $F(x)$ can always be derived from a potential $V(x)$, according to

$$F(x) \;=\; -\;\frac{\partial}{\partial x}\,V(x) \tag{13}$$

For instance, in the harmonic case, $V(x) = \frac{1}{2}\,k_0x^2$. However, we are interested in the general nonharmonic case. We assume a force that, besides a harmonic linear term has a cubic dependence on the coordinate:

$$F(x) \;=\; -\,k_0x \;-\; k_1x^3 \tag{14}$$

that derives from a quartic potential

$$V(x) \;=\; \frac{1}{2}\, k_0 x^2 \;+\; \frac{1}{4}\, k_1 x^4. \tag{15}$$

The form of the potential is depicted in Fig.4. In part (i) we show the case $k_0 > 0$, while the case $k_0 < 0$ is shown in part (ii). The equilibrium points will be determined from $F(x) = 0$. From the figure it is clear that in each

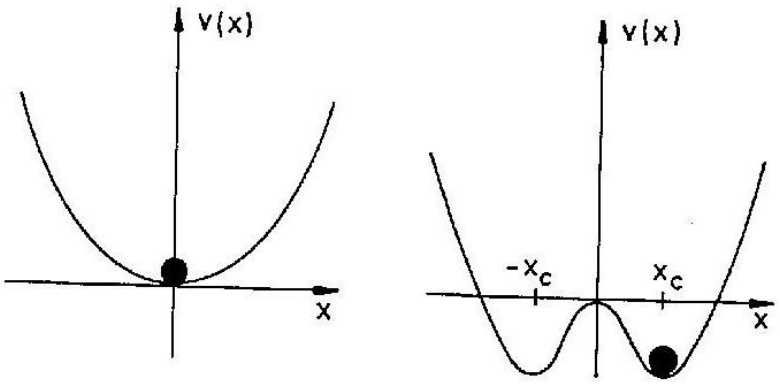

Fig. 4. Schematic quartic potential.

In the first case, for $k_0 > 0$ and $k_1 > 0$, the unique solution is $x = 0$, and is stable; whereas in the second, for $k_0 < 0$ and $k_1 > 0$, we have three solutions, namely, $x = 0$ which is unstable, and two stable symmetric solutions $x = \pm x_c$ (where $x_c = [\mid k_0 \mid /k_1]^{1/2}$). Here we meet again the *bifurcation* phenomenon discussed above.

It is easy to prove, within linear stability analysis, that both solutions $x = \pm x_c$, are stable. Also, it is simply proven that (12) with $F(x)$ given by (14) is invariant under the transformation $x \to -x$, that is, (12) is symmetric with respect to this transformation. Also the potential in (15) remains invariant under such a transformation. Although the problem, as described by (12) and (14) is completely symmetric under inversion, the symmetry is now broken as the system will adopt one of the two possible solutions. We then have that, when we slowly change k_0 from positive to negative values, we reach $k_0 = 0$ where the stable equilibrium solution $x = 0$ becomes unstable. This phenomenon is usually described as a *symmetry breaking instability.* ([63, 23, 68, 62])

2.4 Lyapunov Functional, Global Stability

We can extend the previous results to higher dimensional situations to conclude that, when there is a potential function $V(x_1, .., x_n)$ from which we can derive the forces

$$F_j(x_1,..,x_n) \;=\; -\frac{\partial}{\partial x_j}V(x_1,..,x_n), \tag{16}$$

we can discuss the stability of the steady state solutions just by looking at the form of the potential. In other words, we have a *global stability criterion*. However, there are a large majority of systems which do not have such a potential. There is a theorem due to *Lyapunov* stating that, if certain conditions are fulfilled, there exists a function which has the desirable properties making it possible to discuss global stability. Such function is not based on the requirement that the forces be derived from a potential, i.e. the system could be *non-variational* (that means: (16) is not fulfilled).

To fix ideas, in the two variable case indicated in (5), Lyapunov's theorem states that: if there exists a function $V(x_1,x_2)$ such that it has a minimum at the fixed point $(\bar{x_1},\bar{x_2})$, in the neighborhood of this fixed point and both $V(x_1,x_2)>0$ and $\mathrm{d}V(x_1,x_2)/\mathrm{d}t \leq 0$, then such a fixed point will be asymptotically stable. ([69, 43, 62])

At this point, and with the idea of the Lyapunov function in mind, it is worth to make a brief classification of the different possibilities for the flow in the phase space. ([30, 19, 20, 8, 55]) [3]

(i) *Relaxational Gradient Flow:* If there is a potential function $V(x_1,..,x_n)$ such that $F_j(x_1,..,x_n)$ fulfills (16) (i.e., it is a variational system), implying

$$\dot{x}_j \;=\; -\frac{\partial}{\partial x_j}V(x_1,..,x_n), \tag{17}$$

where the fixed points will correspond to the extreme of $V(x_1,..,x_n)$, the phase space flow will correspond to what is called a *relaxational gradient flow*, and the system will evolve towards the minimum of $V(x_1,..,x_n)$ following trajectories that correspond to the line of *steepest descent*. Clearly $V(x_1,..,x_n)$ is a Lyapunov functional as it also fulfills

$$\frac{\mathrm{d}V}{\mathrm{d}t} \;=\; \sum \frac{\partial V}{\partial x_j}\frac{\mathrm{d}x_j}{\mathrm{d}t} \;=\; -\sum(\frac{\partial V}{\partial x_j})^2 \;\leq\; 0. \tag{18}$$

This behavior is depicted in part (a) of Fig.5.

(ii) *Relaxational non-Gradient Flow:* Consider a system governed by the equation

$$\dot{x}_j \;=\; -\sum(\mathbb{T})_{jl}\frac{\partial V}{\partial x_l}, \tag{19}$$

where $\mathbb{T}$ is a real, symmetric, positive definite matrix. The fixed points of the system will still correspond to the extreme of V. However, the trajectories in phase space that will evolve towards the minima of V, will not follow the steepest descent lines. This means that the transient dynamics will not

[3] I am indebted to Raul Toral for this presentation of the classification of flows in phase space.

be governed just by V. A, by now, classical example of this situation is the Cahn-Hilliard equation for spinodal decomposition, ([45, 30, 22, 71, 41, 8]) where $(\mathbb{T})_{jl} = -\nabla^2$.

It is clear that V is still a Lyapunov functional as

$$\frac{\mathrm{d}V}{\mathrm{d}t} = \sum (\mathbb{T})_{jl} \frac{\partial V}{\partial x_j} \frac{\partial V}{\partial x_l} \leq 0. \tag{20}$$

This behavior is depicted in part (b) of Fig.5.

(iii) *Non-Relaxational Potential Flow:* Here we can consider two situations:
(a) In the first case we assume

$$\dot{x}_j = -\sum (\mathbb{IK})_{jl} \frac{\partial V}{\partial x_l}, \tag{21}$$

Where $\mathbb{IK}$ is an arbitrary, positive definite matrix. We can separate it into a symmetric ($\mathbb{S}$) and an antisymmetric ($\mathbb{IF}$) part

$$\begin{aligned} \mathbb{IK} &= \mathbb{S} + \mathbb{IF} \\ \mathbb{S} &= \frac{1}{2}(\mathbb{IK} + \mathbb{IK}^T) \quad \mathbb{S} = \mathbb{S}^T \\ \mathbb{IF} &= \frac{1}{2}(\mathbb{IK} - \mathbb{IK}^T) \quad \mathbb{IF} = -\mathbb{IF}^T. \end{aligned} \tag{22}$$

The fixed points are again given by the extreme of V. On the other hand we have that V also fulfills

$$\frac{\mathrm{d}V}{\mathrm{d}t} = \sum (\mathbb{S})_{jl} \frac{\partial V}{\partial x_j} \frac{\partial V}{\partial x_l} - \sum (\mathbb{IF})_{jl} \frac{\partial V}{\partial x_j} \frac{\partial V}{\partial x_l} \leq 0, \tag{23}$$

as, clearly, the first term on the rhs is ≤ 0, while the second one is $= 0$. Hence V is again a Lyapunov function. The later result implies that the antisymmetric part of $\mathbb{IK}$ induces a flow in the system that keeps the Lyapunov functional constant (that is *without cost*). A typical situation is depicted in part (c) of Fig.5.

(b) In the second case we consider

$$\dot{x}_j = f_j = -\sum (\mathbb{T})_{jl} \frac{\partial V}{\partial x_l} + w_j, \tag{24}$$

with $(\mathbb{T})_{jl}$ as in (ii) and w_j an arbitrary function. In the present case, $V(x_1, x_2, ...)$ will be a Lyapunov functional if the second term on the rhs of

$$\frac{\mathrm{d}V}{\mathrm{d}t} = -\sum (\mathbb{T})_{jl} \frac{\partial V}{\partial x_j} \frac{\partial V}{\partial x_l} + \sum w_j \frac{\partial V}{\partial x_j} \tag{25}$$

is zero. For this to be true, the following orthogonality condition must be fulfilled

$$\sum_l \left(f_l \; + \; \sum_j (\mathbb{T})_{jl} \frac{\partial V}{\partial x_j} \right) \; \frac{\partial V}{\partial x_l} \; = \; 0, \tag{26}$$

or

$$(\boldsymbol{F} \; + \; \mathbb{T} \; \nabla V) \; . \nabla V \; = \; 0, \tag{27}$$

that is analogous to a Hamilton-Jacobi equation. In such a case we have that $\frac{dV}{dt} \leq 0$ and V is a Lyapunov function.

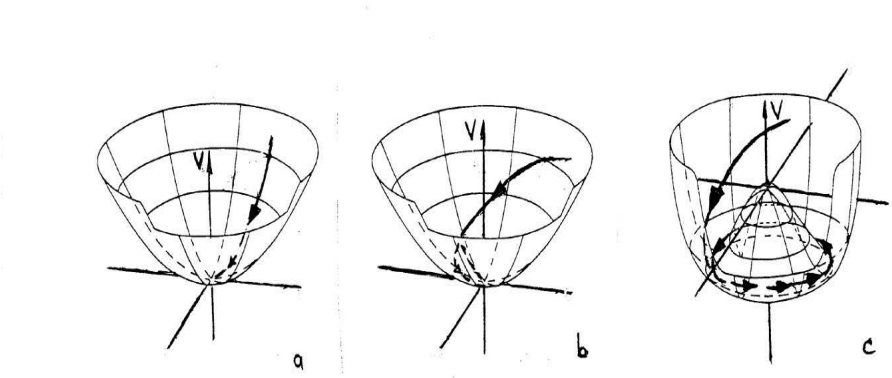

Fig. 5. (a) Case i); (b) case ii) and (c) case iii).

A more general discussion on such a classification of dynamical flows for complex fields can be found in [55].

At this point it is worth asking about the effect of noise or fluctuations on the dynamical equation (12) as well as on the stability of the fixed points. Before analyzing this problem, we will proceed to make a brief review on some aspects of stochastic processes.

3 Stochastic Processes: A Brief Overview

We start this section by rewriting equation (1) for the one dimensional case:

$$\frac{\mathrm{d}x}{\mathrm{d}t} = F(x, \zeta) \tag{28}$$

where x corresponds to the state variable while ζ is a control parameter. For instance, such a parameter could be the temperature, an external field, a reactant's controlled flux, etc, indicating the form in which the system is coupled to its surroundings. Experience tells us that it is usually impossible to keep fixed the value of such parameters, and consequently that its fluctuations become relevant. Hence, the original *deterministic* equation will acquire a random or *stochastic* character.

Among the many reasons to justify the increasing interest in the study of fluctuations we can quote that they present a serious impediment to accurate measurements in very sensitive experiments, demanding some very specific techniques in order to reduce their effects. Besides, the fluctuations might be used as an additional source of information about the system. But the most important aspect is that fluctuations can produce macroscopic effects contributing to the appearance of *spatio-temporal patterns* or *dissipative structures*. ([31, 60, 61, 11, 82])

The general character of equations (1) makes it clear why stochastic methods have become so important in different branches of physics, chemistry, biology, technology, population dynamics, economy, and sociology. In spite of the large number of different problems that arise in all these fields, there are some common principles and methods that are included in a common framework: the theory of stochastic processes. Here we will only briefly review the few aspects relevant for our present needs. For deeper study we refer to ([76, 70, 17, 31, 11, 82]).

In order to introduce the presence of fluctuations into our description, we write $\zeta = \zeta_0 + \xi(t)$, where ζ_0 is a constant value and $\xi(t)$ is the random or fluctuating contribution to the parameter ζ. The simplest (or lowest order) form that equation (28) can adopt is

$$\frac{\mathrm{d}x}{\mathrm{d}t} = \dot{x} = F(x, \zeta_0) + g(x, \zeta_0)\xi(t), \tag{29}$$

The original deterministic differential equation has been transformed into a *stochastic differential equation* (SDE), where $\xi(t)$ is called a *noise* term or stochastic process.

Any stochastic process $x(t)$ is completely specified if we have have the information of the complete hierarchy of probability densities. We write

$$P_n(x_1, t_1;\ x_2, t_2; ...;\ x_n, t_n)\ \mathrm{d}x_1\ \mathrm{d}x_2\ ...\mathrm{d}x_n, \tag{30}$$

for the probability that $x(t_1)$ is within the interval $(x_1, x_1 + \mathrm{d}x_1), x(t_2)$ in $(x_2, x_2 + \mathrm{d}x_2)$, and so on. These P_n may be defined for $n = 1, 2, ...$, and only for different times. This hierarchy fulfills some properties
i) $P_n \geq 0$
ii) P_n is invariant under permutations of pairs (x_i, t_i) and (x_j, t_j)
iii) $\int P_n\ \mathrm{d}x_n = P_{n-1}$, and , $\int P_1\ \mathrm{d}x_1 = 1$.

Another important quantity is the *conditional probability density* $P_{n/m}$ that corresponds to the probability of having the value x_1 at time t_1, x_2 at $t_2, \ldots, x_n$ at t_n; given that we have $x(t_{n+1}) = x_{n+1}, x(t_{n+2}) = x_{n+2}, x(t_{n+3}) = x_{n+3}, \ldots, x(t_{n+m}) = x_{n+m}$. Its definition is

$$\begin{aligned} P_{n/m}(x_1,\ t\ _1; ..; x_n, t_n \mid x_{n+1}, t_{n+1}; ..; x_{n+m}, t_{n+m}) \ &= \\ = \ P_{n+m}(x_1, t_1; \ldots; x_n, t_n; x_{n+1}, t_{n+1}; ...; x_{n+m}, t_{n+m}) & \\ (P_m(x_{n+1}, t_{n+1}; ..; x_{n+m}, t_{n+m}))^{-1} & \end{aligned} \tag{31}$$

Among the many possible classes of stochastic processes, there is one that plays a central role: *Markovian Processes.* ([76, 70, 17, 31, 11, 82]) For a stochastic process $x(t), P(x_2, t_2 \mid x_1, t_1)$ is the *conditional* or *transition* probability that $x(t_2)$ takes the value x_2, knowing that $x(t_1)$ has taken the value x_1. From this definition and (31) results the following identity for the *joint probability* $P_2(x_1, t_1; x_2, t_2)$ (Bayes' rule) :

$$P_2(x_1, t_1; x_2, t_2) \;=\; P(x_2, t_2 \mid x_1, t_1)\; P_1(x_1, t_1). \tag{32}$$

A process $x(t)$ is called *Markovian* if for every set of successive times $t_1 < t_2 < .. < t_n$, the following condition holds

$$\begin{aligned} P_n(x_1,\, t_1\, , \ldots, x_n, t_n) &= P_1(x_1, t_1) P_{n-1}(x_2, t_2, \ldots, x_n, t_n \mid x_1, t_1) \\ &= \; P_1(x_1, t_1)\; P(x_n, t_n \mid x_{n-1}, t_{n-1}) ... P(x_2, t_2 \mid x_1, t_1), \end{aligned} \tag{33}$$

From this definition, it results that a Markovian process is completely determined if we know $P_1(x_1, t_1)$ and $P(x_2, t_2 \mid x_1, t_1)$. It is easy to find a relevant condition to be fulfilled for Markovian processes: specifying the previous equation for the case $n = 3$ and integrating over x_2, we obtain

$$\begin{aligned} \int \mathrm{d}x_2\; P_3(\; x_1\; , t_1, x_2, t_2, x_3, t_3) \;&=\; P_2(x_1, t_1, x_3, t_3) \\ &=\; P_1(x_1, t_1)\; P(x_3, t_3 \mid x_1, t_1) \\ &=\; \int \mathrm{d}x_2\; P_1(x_1, t_1)\; P(x_3, t_3 \mid x_2, t_2)\; P(x_2, t_2 \mid x_1, t_1). \end{aligned} \tag{34}$$

For $t_1 < t_2 < t_3$ we find the identity

$$P(x_3, t_3 \mid x_1, t_1) \;=\; \int \mathrm{d}x_2\; P(x_3, t_3 \mid x_2, t_2)\; P(x_2, t_2 \mid x_1, t_1), \tag{35}$$

which is the *Chapman-Kolmogorov Equation* for Markovian processes. Every pair of non-negative functions $P_1(x_1, t_1)$ and $P(x_2, t_2 \mid x_1, t_1)$, adequately normalized and satisfying not only (35) but also

$$P_1(x_2, t_2) \;=\; \int \mathrm{d}x_1\; P_1(x_1, t_1)\; P(x_2, t_2 \mid x_1, t_1), \tag{36}$$

defines a Markovian process. Some typical (useful) examples of Markov processes are: the *Wiener-Levy*, the *Ornstein-Uhlenbeck* and the *Poisson* processes. ([76, 70, 17, 31, 11, 82])

The Chapman-Kolmogorov equation (that is only a property of the solution for Markovian processes) can be recast into a useful form. Returning to (35), we take $t_3 = t_2 + \delta t$ and consider the limit $\delta t \to\; 0$. It is clear that we have $P(x_3, t_3 \mid x_2, t_2) = \delta(x_3 - x_2)$, and it is intuitive to assume that, if $t_3 - t_2 \simeq \delta t$ (very small), the probability that a transition happens must be proportional to δt. According to this we adopt

$$P(x_3, t_2+\delta t \mid x_2, t_2) \;=\; \delta(x_3-x_2)\;[1 - A(x_2)\;\delta t] \;+\; \delta t\, W(x_3 \mid x_2) \;+O(\delta t^2), \tag{37}$$

where $W(x_3 \mid x_2)$ is the *transition probability per unit time* from x_2 to x_3 (which in general could also be a function of t_2). The probability normalization tells us that

$$A(x_2) \;=\; \int W(x_3 \mid x_2)\; \mathrm{d}x_3$$

Substitution of the form for $P(x_3, t_2 + \delta t \mid x_2, t_2)$ into (35) gives

$$\begin{aligned} P\;(\;x_3, t_2 + \delta t \mid x_1, t_1) \;&=\; \int P(x_3, t_2 + \delta t \mid x_2, t_2)\; P(x_2, t_2 \mid x_1, t_1)\; \mathrm{d}x_2 \\ &= [1 - A(x_3)\;\delta t]\; P(x_3, t_2 \mid x_1, t_1) \;+\; \delta t \int W(x_3 \mid x_2)\; P(x_2, t_2 \mid x_1, t_1)\; \mathrm{d}x_2 \\ &= P(x_3, t_2 \mid x_1, t_1) \;-\; \delta t \int W(x_2 \mid x_3)\; P(x_3, t_2 \mid x_1, t_1)\; \mathrm{d}x_2 \\ &\quad + \delta t \int W(x_3 \mid x_2)\; P(x_2, t_2 \mid x_1, t_1)\; \mathrm{d}x_2. \end{aligned} \tag{38}$$

This can be rearranged as

$$\begin{aligned} [P(x_3, t_2 + \delta t \mid x_1, t_1) - P(x_3, t_2 \mid x_1, t_1)]/\delta t = \int [W(x_3 \mid x_2) P(x_2, t_2 \mid x_1, t_1) \\ - W(x_2 \mid x_3) P(x_3, t_2 \mid x_1, t_1)]\, \mathrm{d}x_2, \end{aligned} \tag{39}$$

and in the limit $\delta t \to 0$, we find

$$\begin{aligned} \frac{\partial}{\partial t}\; P(x, t \mid x_0, t_0) \;=\; \int \quad & [W(x \mid x')\; P(x', t' \mid x_0, t_0) \\ & - \;\; W(x' \mid x)\; P(x, t \mid x_0, t_0)]\, \mathrm{d}x', \end{aligned} \tag{40}$$

which corresponds to the *Master Equation*. ([76, 70, 17, 31, 11, 82])

The master equation is a differential form of the Chapman-Kolmogorov equation. It is an equation for the transition probability $P(x, t \mid x_0, t_0)$, and is more adequate for mathematical manipulations than the Chapman-Kolmogorov equation, and has a direct physical interpretation as a balance equation. At the same time, $W(x \mid x')\delta t$ is the transition probability during a very short time (δt). It could be evaluated by approximate methods, for instance by time dependent perturbation theory (i.e. : the *Fermi golden rule*). ([76, 17, 82])

3.1 Langevin Equations

Brownian motion is the oldest and best known physical example of a Markov process. This phenomenon corresponds to the motion of a heavy test particle, immersed in a fluid composed of light particles in random motion. Due to

the (random) collisions of the light particles against the test particle, the velocity of the latter varies in a (large) sequence of small, uncorrelated jumps. However, similar ideas can (and have) been applied to a large variety of systems. ([79, 4, 76, 43, 17, 82]) To simplify the presentation we restrict the description to a one dimensional system.

We will give a simple quantitative picture of Brownian motion. We start by writing the Newton equation as :

$$m\,\dot{v} \;=\; F(t) \;+\; f(t), \tag{41}$$

where m is the mass of the Brownian particle, v its velocity, $F(t)$ the force due to some external field (i.e. gravitational, electrical for charged particles, etc), and $f(t)$ is the force produced by the collisions of fluid particles against the test particle. Due to the above indicated rapid fluctuations in v, we have two effects. On one hand a *systematic* one, i.e., a kind of *friction* that tends to slow down the particle, and on the other hand, a *random* contribution originated in the random hits of the fluid particle. If the mass of the test particle is much larger than the mass of the fluid particles (implying that the fluid *relaxes* faster than the test particle, allowing us to assume that it is in equilibrium), we can write

$$\frac{1}{m} f(t) \;=\; -\;\gamma\, v \;+\; \xi(t). \tag{42}$$

In the r.h.s., γ is the friction coefficient, and the minus sign in the first term indicates that this contribution (as a good friction term) opposes the motion. The second term corresponds to the stochastic or random contribution, since we have separated the systematic contribution in the first term, and this random contribution averages to zero : $\langle \xi(t) \rangle \;=\; 0$ (where the average is over an *ensemble* of noninteracting Brownian particles). In order to define the so called *Langevin force* (or *white noise*) it is required that

$$\langle \xi(t)\xi(t') \rangle = \; D\;\delta(t-t'). \tag{43}$$

We will not consider higher order moments, but it is clear that to fully characterize the fluctuating force, we need the whole hierarchy of moments. ([76, 17, 82])

With the above indicated arguments, and without an external field, (41) adopts the form

$$\dot{v} \;=\; -\;\gamma\, v \;+\; \xi(t), \tag{44}$$

which is known as the *Langevin equation*. ([76, 70, 17, 31, 11, 82]). This is the simplest example of a SDE (that is, a differential equation whose coefficients are random functions with known stochastic properties). Hence $v(t)$ is a stochastic process, with a given initial condition. For details we refer the reader to ([76, 70, 17, 31, 11, 82]).

When an external field is present, we have the pair of equations

$$\begin{aligned} \dot{x} &= v \\ \dot{v} &= \frac{1}{m}F(x) - \gamma\, v + \xi(t). \end{aligned} \tag{45}$$

After differentiating the first one and replacing the second, it adopts the form

$$\ddot{x} = \frac{1}{m}F(x) - \gamma\, \dot{x} + \xi(t). \tag{46}$$

In the case of large friction (γ very large), through an *adiabatic elimination* ($\ddot{x} \simeq 0$, as in Sect.2.3), ([23, 76, 17, 11, 82]) we can rewrite the last equation as

$$\dot{x} = -\frac{\partial}{\partial x}\, V(x) + \xi(t), \tag{47}$$

where $\frac{\partial}{\partial x}\, V(x) = -F(x)$, and m and γ have been absorbed into the different terms. The last result corresponds to the problem of *diffusion in a field*. ([76, 70, 17, 31, 11, 82])

The most general form of the SDE that we will consider here is the one indicated by equation (29).

3.2 Fokker-Planck Equations

Let us return to the Master Equation (40). We assume that x is a continuous variable, and that its changes correspond to *small jumps* (or variations). In this case it is possible to derive, starting from the Master Equation, a differential equation. The transition probability $W(x \mid x')$ will decay very fast as a function of $\mid x - x' \mid$. We could then write $W(x \mid x') = W(x', \xi)$, where $\xi = x - x'$ corresponds to the size of the jump. The Master Equation will take the form

$$\begin{aligned} \frac{\partial}{\partial t}\, P(x,t \mid x_0,t_0) = & \int W(x-\xi,\xi)P(x-\xi,t \mid x_0,t_0)\mathrm{d}\xi \\ & - P(x,t \mid x_0,t_0)\int W(x,-\xi)\mathrm{d}\xi. \end{aligned} \tag{48}$$

Following our the assumption of small jumps, and the additional argument that P varies slowly with x, we make a Taylor expansion in ξ that gives

$$\begin{aligned} \frac{\partial}{\partial t}\, P(x,t \mid x_0,t_0) = \int \Big[& W(x,\xi)\; P(x,t \mid x_0,t_0) - \xi\frac{\partial}{\partial x}W(x,\xi)\; P(x,t \mid x_0,t_0) \\ & + \xi^2\; \frac{\partial^2}{\partial x^2}W(x,\xi)\; P(x,t \mid x_0,t_0) - ... \Big]\, \mathrm{d}\xi \\ & - P(x,t \mid x_0,t_0)\; \int W(x,-\xi)\mathrm{d}\xi. \end{aligned} \tag{49}$$

As the first and the last terms are equal (in the latter changing $-\xi$ by ξ, as well as the integration limits), we get

$$\frac{\partial}{\partial t}\, P(x,t \mid x_0,t_0) \;=\; \sum_{\nu=1}^{\infty} \frac{(-1)^\nu}{\nu!}\, \frac{\partial^\nu}{\partial x^\nu}\, \alpha_\nu(x)\; P(x,t \mid x_0,t_0), \tag{50}$$

with $\alpha_\nu(x) = \int \xi^\nu\; W(x,\xi)\mathrm{d}\xi$. This result corresponds to the *Kramers-Moyal expansion* of the Master Equation. ([76, 70, 17, 31, 11, 82]) Up to this point we have gained nothing. However, there could be situations where, for $\nu > 2$, the α_ν are either zero or very small (even though there are no *a priori* criteria about the relative size of the terms). If this is the case, we have

$$\begin{aligned}\frac{\partial}{\partial t} P(x,t \mid x_0,t_0) = &- \frac{\partial}{\partial x}\alpha_1(x)\; P(x,t \mid x_0,t_0) \\ &+ \frac{1}{2}\, \frac{\partial^2}{\partial x^2}\; \alpha_2(x)\; P(x,t \mid x_0,t_0),\end{aligned} \tag{51}$$

which corresponds to the *Fokker-Planck equation*. ([76, 70, 17, 31, 11, 82])

Let us see a couple of examples. For the Wiener-Levy process we find that $\alpha_\nu = 0$ ($\nu > 2$), and then

$$\frac{\partial}{\partial t}\, P(x,t \mid x_0,t_0) \;=\; \frac{\partial^2}{\partial x^2}\; P(x,t \mid x_0,t_0),$$

while for the case of the Ornstein-Uhlenbeck process we get

$$\frac{\partial}{\partial t}\, P(x,t \mid x_0,t_0) \;=\; -\; \frac{\partial}{\partial x}\; x\; P(x,t \mid x_0,t_0) \;+\; \frac{\partial^2}{\partial x^2}\; P(x,t \mid x_0,t_0).$$

Equation (51) corresponds to a *nonlinear* Fokker-Planck equation (due to the dependence of $\alpha_1(x)$ and $\alpha_2(x)$ on x), which is the result of poorly grounded assumptions (i.e., the criteria to decide where to cut the expansion, etc). Even worse, it is **not a systematic** approximation to the Master Equation. However, there is a procedure due to van Kampen that does make it possible to build up such a systematic procedure, but we will not discuss it here and instead refer the reader to ([76, 17, 82]).

Consider the long time limit, where we expect that the system will reach a stationary behavior (that is: $\frac{\partial}{\partial t} P(x,t \mid x_0,t_0) = 0$). In such a case we will have that

$$0 \;=\; -\; \frac{\mathrm{d}}{\mathrm{d}x}\alpha_1(x)\; P_{st}(x) \;+\; \frac{D}{2}\; \frac{\mathrm{d}^2}{\mathrm{d}x^2}\; P_{st}(x), \tag{52}$$

where in order to simplify we have taken $\alpha_2(x) = \text{ct.} = D$. The stationary distribution turns out to be

$$P_{st}(x) \;\simeq\; \mathcal{N}\mathrm{e}^{-\int \mathrm{d}x'\alpha_1(x')/D}. \tag{53}$$

The exponent in the last equation allows us to define the *(nonequilibrium) potential* $U(x)$ through

$$U(x) \;=\; -\int \mathrm{d}x'\alpha_1(x'). \tag{54}$$

3.3 Connection Between LE and FPE.

Here we give a brief and more or less formal (but not completely rigorous from a mathematical point of view) presentation of the relation between *stochastic differential equations* (SDE) of the *Langevin type* (LE), and *Fokker-Planck equations* (FPE). We start considering a general form for the one-dimensional SDE as indicated in (29):

$$\dot{x}(t) \;=\; \frac{\mathrm{d}x(t)}{\mathrm{d}t} \;=\; f[x(t),t] \;+\; g[x(t),t]\;\xi(t) \tag{55}$$

where $\xi(t)$ is a *white noise* with

$$\langle\; \xi(t)\;\rangle \;=\; 0 \quad \text{and} \quad \langle\; \xi(t)\;\xi(t')\;\rangle \;=\; \delta(t-t')$$

as in (42) and (43), with $D = 1$. We made the usual assumption that the process is Gaussian. However, $\xi(t)$ is not a well defined stochastic process. In a loose way, it could be considered as the derivative of the well defined *Wiener process*, but such a derivative does not exist at all. ([76, 17, 11, 82]) We now integrate (55) over a short time interval δt

$$x(t+\delta t) \;-\; x(t) \;=\; f[x(t),t]\;\delta t \;+\; g[x(t),t]\;\xi(t)\;\delta t \tag{56}$$

As $x(t)$ is a Markov process, it is well defined if we are able to determine its probability distribution $P_1(x,t)$ as well as its conditional probability distribution $P(x,t \mid x',t')(t \;>\; t')$. In order to obtain an equation for the latter quantity, we define now a *conditional average*, corresponding to the average of a function of the stochastic variable x (say $F(x)$), given that x has the value y at $t' \;<\; t$:

$$\langle F(x(t)) \mid x(t') = y\rangle \;=\; \ll F(x(t) \gg \;=\; \int \mathrm{d}x' F(x')\; P(x',t \mid y,t'). \tag{57}$$

Due to the property $P(x,t \mid x',t) \;=\; \delta(x-x')$, we have

$$\langle F(x(t)) \mid x(t) = y\rangle \;=\; F(y). \tag{58}$$

We use now this definition in order to obtain the first few *conditional moments* of $x(t)$.

$$\begin{aligned} \ll \Delta x(t) \gg = \langle x(t+\delta t) \mid x(t) = x\rangle \;= \\ = \ll\; f[x(t),t]\;\delta t \;\gg \;+\; \ll g[x(t),t]\;\xi(t)\;\delta t \;\gg . \end{aligned} \tag{59}$$

The result shown in (58) indicates that $\ll f[x(t),t]\;\delta t \gg \;=\; f[x(t),t]\;\delta t$, and also that $\ll g[x(t),t]\;\xi(t)\;\delta t \gg = g[x(t),t]\;\ll \xi(t) \gg \delta t = 0$, resulting in

$$\ll \Delta x(t) \gg \;=\; f[x(t),t]\;\delta t. \tag{60}$$

For the second moment we need to resort to properties of the Wiener process; i.e. using that $\xi(t)\ \delta t\ =\ \int_t^{t+\delta t} \mathrm{d}t\xi(t')\ =\ \Delta W(t)$, where $W(t)$ is the Wiener process, and $\langle[\xi(t)\ \delta t]^2\rangle\ \simeq\ \langle \Delta W(t)^2\rangle\ =\ \Delta t$; to obtain

$$\ll \Delta x(t)^2 \gg\ =\ g[x(t),t]^2\delta t\ +\ O(\delta t^2). \tag{61}$$

Let us now consider an arbitrary function $R(x)$, and evaluate its conditional average. Using the Chapman-Kolmogorov equation

$$\int \mathrm{d}x\ R(x)\ P(x,t+\delta t\mid y,s) = \int \mathrm{d}z\ P(z,t\mid y,s) \int \mathrm{d}x\ R(x)\ P(x,t+\delta t\mid z,t), \tag{62}$$

We can expand $R(x)$ in a Taylor series around z, as for $\delta t \simeq 0$ we know that $P(x,t+\delta t\ \mid\ z,t)\ \simeq\ \delta(x-z)$, and that only a neighborhood of z will be relevant. If we also remember the normalization condition for $P(z,t\mid y,s)$, integrate by parts and use (60) and (61) we obtain an equation that, after arranging terms and taking the limit $\delta t \to 0$, gives

$$\int \mathrm{d}x\ R(x)\ \Big(\frac{\partial}{\partial t}\ P(x,t\ \mid\ y,s) - \big(-\frac{\partial}{\partial x}\ [f[x,t]\ P(x,t\ \mid y,s)] + \frac{1}{2}\ \frac{\partial^2}{\partial x^2}\ \big[g(x,t)^2\ P(x,t\ \mid y,s)\big]\big)\Big)\ =\ 0 \tag{63}$$

Due to the arbitrariness of the function $R(x)$, we arrive at the condition

$$\frac{\partial}{\partial t}\ P(x,t\ \mid y,s)\ =\ -\ \frac{\partial}{\partial x}\ \{f[x,t]\ P(x,t\ \mid y,s)\} + \frac{1}{2}\ \frac{\partial^2}{\partial x^2}\ \{g(x,t)^2\ P(x,t\ \mid y,s)\} \tag{64}$$

which is the desired Fokker-Planck equation for the transition probability $P(x,t\mid y,s)$ associated with the stochastic process driven by the SDE (55).

3.4 Decay Times: Kramers Result

Here we want to discuss how, due to the influence of fluctuations, it is possible that transitions from metastable states into more stable states can occur and how to describe this process.

Let us start considering the problem described by the LE (55) or the FPE (64), but assuming the simple case where $g(x,t)^2 = D$ and $f(x,t) = f(x) = -\frac{\partial}{\partial x}U(x)$, with $U(x) = \frac{k}{2}x^2$. The FPE adopts the form

$$\frac{\partial}{\partial t}\ P(x,t\ \mid y,0)\ =\ \frac{\partial}{\partial x}\ \Big([\frac{\partial}{\partial x}U(x)]\ P(x,t\ \mid y,0)\Big) + \frac{D}{2}\ \frac{\partial^2}{\partial x^2}\ P(x,t\ \mid y,0). \tag{65}$$

For $t \to 0$, we have that $\lim P(x,t \mid y,0) \to \delta(x-y)$, and for very long times $(t \to \infty)$ we find the stationary distribution

$$P_{st}(x) \;=\; C\ \mathrm{e}^{-U(x)/D} \quad ; \quad C^{-1} = \int \mathrm{d}x' \mathrm{e}^{-U(x')/D}. \tag{66}$$

When $U(x)$ is not the quadratic potential indicated above but is still monostable (with the minimum in $x = a$) we can approximately write it as in (66)

$$P_{st}(x) \;\simeq\; \Big(\frac{U"(a)}{2\pi D}\Big)^{1/2}\ \mathrm{e}^{-\frac{U"(a)}{2D}(x-a)^2}, \tag{67}$$

with $U"(a) = \frac{\partial^2}{\partial x^2} U(x)|_{x=a}$. Clearly, it is also an approximation to the form of $P_{st}(x)$ for a *bistable* potential, near one of the minima. See, as an example, the sketch in Fig.(6)

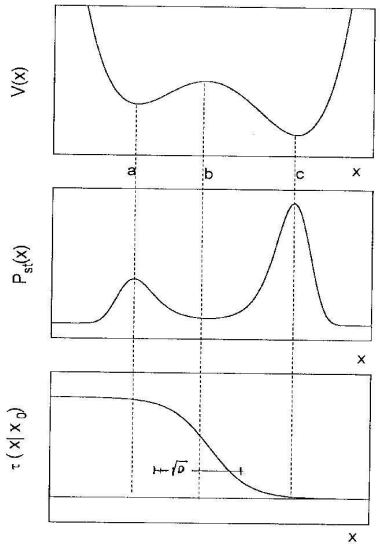

Fig. 6. (i) Bistable potential, (ii) stationary distribution, (iii) decay time.

We can describe the probability of being in the left or in the right well as:

$$\Xi_a(t) = \int_{\Omega(a)} P(x,t)\mathrm{d}x \tag{68}$$

$$\Xi_c(t) = \int_{\Omega(c)} P(x,t)\mathrm{d}x, \tag{69}$$

where $\Omega(a)$ and $\Omega(c)$ indicates the set of points in the attraction basin of the minimum at $x = a$ and c respectively. Clearly, the probabilities $\Xi_i(t)$ fulfill the normalization condition $\Xi_a(t) + \Xi_c(t) = 1$. Hence, calling τ_{ij} the inverse of the transition probability per unit time from j to i, we can write the kinetic equations

$$\frac{\mathrm{d}}{\mathrm{d}t}\Xi_a(t) = -\frac{\Xi_a}{\tau_{ca}} + \frac{\Xi_c}{\tau_{ac}} = -\frac{\mathrm{d}}{\mathrm{d}t}\Xi_b(t), \tag{70}$$

that have the stationary solutions

$$\begin{aligned} \Xi_a^{st} &= \frac{\tau_{ac}}{\tau_{ac} + \tau_{ca}} \\ \Xi_c^{st} &= \frac{\tau_{ca}}{\tau_{ac} + \tau_{ca}}. \end{aligned} \tag{71}$$

Exploiting the Gaussian approximation (67) we also have

$$P_{st}(x) = \Xi_a^{st}\Big(\frac{U"(a)}{2\pi D}\Big)^{1/2}\,\mathrm{e}^{-\frac{U"(a)}{2D}(x-a)^2} + \Xi_c^{st}\Big(\frac{U"(c)}{2\pi D}\Big)^{1/2}\,\mathrm{e}^{-\frac{U"(c)}{2D}(x-c)^2}, \tag{72}$$

from which we can obtain the ratio

$$\frac{\Xi_a^{st}}{\Xi_c^{st}} = \frac{\tau_{ac}}{\tau_{ca}} = \Big(\frac{U"(c)}{U"(a)}\Big)^{1/2}\,\mathrm{e}^{-\frac{[U(a)-U(c)]}{D}}. \tag{73}$$

The exponential factor has the form of an *Arrhenius* factor that arises in the evaluation of reaction probabilities or its inverse, the characteristic decay time, for activation processes. ([69, 76, 43, 71, 39, 25]) However, through this procedure we can only obtain the indicated ratio. More elaborate calculations based on Kramers-like approaches ([76, 17, 25]) yields for the average decay or transition time from the state a to the state c

$$\tau_{ca} = \Big(\frac{2\pi}{U"(a)|U"(b)|}\Big)^{1/2}\,\mathrm{e}^{\frac{[U(b)-U(a)]}{D}}, \tag{74}$$

that is known as *Kramers' formula* (or also *Arrhenius law*). However this expression has some constraints that we can summarize in the following points: the large damped limit was used, and the barrier height must be larger than the fluctuations ($U(b) - U(a) \gg D$). A typical behavior of $\tau(x|x_0)$, that is the escape or decay time from x_0 to x, is depicted in part (iii) of Fig.(6).

For details of the calculation of decay (or *first passage times*) we refer the reader to ([76, 70, 17, 31, 11, 25]).

3.5 Notions of Stochastic Resonance

One of the most fascinating cooperative effects arising out of the interplay between deterministic and random dynamics in a nonlinear system is the

phenomenon of *stochastic resonance* (SR). This phenomenon is characterized by the enhancement of the signal-to-noise ratio (SNR) caused by injection of noise into a periodically modulated nonlinear system. The increase in the noise intensity from small initial values induces an increase in the SNR ratio until it reaches a maximum, beyond which there is a decay of SNR for large noise values. Some recent reviews and conference proceedings clearly show the wide interest of this phenomenon and the state of the art. ([56, 57, 80, 1, 2])

The basic picture of SR has been illustrated by means of a mechanical analogy. Consider a particle moving in a double well potential like the one in Fig.6 and subject to friction. Consider a weak signal that periodically modulates the potential alternatively raising and lowering the wells relative to the barrier. Here weak implies that the modulation is too small to deterministically excite the particle over the barrier. Besides modulation, we also consider the effect of noise, that alone is enough to induce irregular switchings between the wells. In the high friction limit the dynamics can be modelled by

$$\dot{x}(t) \;=\; -\frac{\mathrm{d}U_0(x)}{\mathrm{d}x} + \xi(t) + A\cos\Omega_0 t, \tag{75}$$

where $U_0(x)$ is the bare potential, $A\cos\Omega_0 t$ is the *signal* or modulation and $\xi(t)$ is the random contribution. The phenomenon of SR is the nonlinear cooperative effect whereby the small signal entrains the noise inducing hopping in such a way that the transitions becomes surprisingly regular. Even more, the regularity can improve with the addition of more noise, at least up to a point: it is optimally sensitive at some non-zero level of input noise.

The two essential features of SR in the bistable potential are: that it is a threshold phenomenon, and that its statistical properties are nonstationary. Consider the quartic potential

$$U(x) = U_0(x) + cx = -\frac{a}{2}x^2 + \frac{b}{4}x^4 + cx, \tag{76}$$

with $a, b > 0$ and $c = A\cos\Omega_0 t$. Regarding the threshold feature, the threshold c_{th} is the value of c for which the deterministic switching becomes possible, i.e.: the value of c at which the bistability is destroyed ($c_{th} = \pm[4a^3/27b]^{1/2}$). Hence, weak modulation requires $A < c_{th}$ implying that no deterministic switching can occur with the signal alone. The nonstationarity becomes evident when noise is added, and the potential becomes

$$U(x) = -\frac{a}{2}x^2 + \frac{b}{4}x^4 + x[A\cos\Omega_0 t + \xi(t)].$$

The LE that drives the motion of the particle is

$$\dot{x}(t) \;=\; ax - bx^3 + [A\cos\Omega_0 t + \xi(t)], \tag{77}$$

and non-stationarity means that the probability density is a (periodic) function of time. ([37])

Within the indicated picture, the only important dynamical events are the well-to-well switching transitions that can occur whenever

$$|A\cos\Omega_0 t + \xi(t)| \geq c_{th}, \tag{78}$$

indicating that SR is, fundamentally a threshold phenomenon.

To further clarify the mechanism, let us simplify the picture even more and assume that the modulation is such that during the first half period the left well is kept fixed below the right one, while the situation is reversed during the second half period. Hence, considering the Kramers formula (74), it is clear that, during the first half period, the average decay time for jumping from the right well to the left one will be shorter than the reverse transition. The situation is reversed during the second half period. If the noise intensity is such that this decay time is of the order of half the period (while for the reverse less probable transition it is larger), we will meet a *tuning* condition between the random jumps and the modulation that corresponds to the SR phenomenon.

In order to make a more quantitative description of the phenomenon it is necessary to evaluate the power spectrum of the particle motion in the indicated generic bistable potential (76). To do that, we will follow here McNamara and Wiesenfeld's (MNW) calculation ([50]). We start defining two discrete variables $x_\pm$ describing the position of the particle in either the right $(+)$ or left $(-)$ potential well (for instance, in the indicated bistable potential $x_\pm = \pm[a/b]^{1/2}$), and the corresponding probabilities $\Xi_\pm(t)(\Xi_+(t) = 1 - \Xi_-(t))$. As in the previous section, we can write a rate (or master) equation in terms of $W_\pm$, the transition rates out of the $\pm$ states

$$\frac{\mathrm{d}}{\mathrm{d}t}\Xi_+(t) = -\frac{\mathrm{d}}{\mathrm{d}t}\Xi_-(t) = W_-\Xi_-(t) - W_+\Xi_+(t), \tag{79}$$

which is essentially the same as equation (70) discussed before. Clearly, the only dynamical variables are the particle populations (or probabilities) within the wells, as corresponds to a this approximate two-state dynamics, analogous to the discussion in the previous subsection.

In order to solve (79) at least some approximate form for the $W_\pm$ is required. Following MNW we use an expansion in terms of a small parameter $\eta_0\cos\Omega_0 t$, where $\eta_0 = A/\gamma$ (γ being the noise intensity)

$$W_\pm = \frac{1}{2}\left(\alpha_0 \pm \alpha_1\eta_0\cos\Omega_0 t + \ldots\right), \tag{80}$$

where α_0 and $\alpha_1\eta_0$ are treated as parameters of the system. According to what was discussed in the previous subsection, α_0 and α_1 can be related to the unperturbed Kramers rate (with $r_K \simeq \tau_K^{-1}$) in an adiabatic-like approximation

$$r_K \simeq r_{K,0}\left(1 + \frac{A \mid x_\pm \mid}{\gamma}\cos\Omega_0 t\right). \tag{81}$$

This allows us to express $W_{\pm}$ (within a phase factor) in (79), and to solve it finding a solution $\Xi_{+}(t)$. From this solution we can construct the (conditional) autocorrelation function $\langle x(t)x(t+\tau) \mid x_0, t_0\rangle$, that in the asymptotic limit ($t_o \to -\infty$) yields the desired correlation function $\langle x(t)x(t+\tau)\rangle$. From this last quantity we can obtain the power spectrum through the Wiener-Kintchine theorem ([76, 17, 82]) yielding

$$S(\omega) = \left(1 - \frac{(\alpha_1\eta_0)^2}{2[\alpha_0^2 + \Omega_0^2]}\right)\left(\frac{4\alpha_0\langle x^2\rangle}{[\alpha_0^2 + \omega^2]}\right) + \pi\frac{\langle x^2\rangle(\alpha_1\eta_0)^2}{2[\alpha_0^2 + \Omega_0^2]}\delta(\omega - \Omega_0). \quad (82)$$

This result makes two notable predictions, both borne out by experiment: (i) the shape of the power spectrum is a delta contribution arising from the modulation, riding on a Lorentzian noise background; (ii) the total power -signal plus noise- is a constant. The latter property (that is strictly true only for the bistable model) means that the power in the signal part of the response grows at the expense of the noise power. This result demonstrates that, in such a bistable system, the proper application of noise at the input, can result in more order at the output. This could not be possible with a linear system. Moreover, the nonlinear system must be out of equilibrium.

A quantity that typically has been used to quantify this phenomenon is the *signal-to-noise ratio* (SNR) defined as the ratio between the power from the signal (second term on the rhs of (82)) to the noise power (first term on the rhs of (82), evaluated at $\omega = \Omega_0$). Using the form of the Kramers rate $r_{K,0}$ (inverse of (74)), it is possible to obtain (for the bistable potential) the approximate result

$$\mathrm{SNR} \simeq \left(\frac{A\Delta U_0}{\gamma}\right)^2 \mathrm{e}^{-\Delta U_0/\gamma}, \quad (83)$$

where ΔU_0 is the barrier high: $\Delta U_0 = a^2/4b$. The qualitative form of the power spectral density (psd) and the SNR as function of the noise intensity γ is depicted in Fig.7

The maximum of the curve of SNR results for a value of γ that makes the Kramers time (τ_K) roughly equal to half the period of the modulation. For more details on the SR phenomenon we refer to ([56, 57, 80, 1, 2]).

4 Spatially Extended Systems

Everywhere around us we find examples of *self-organization* or *cooperative phenomena* in *complex systems*, namely the appearance of a relatively simple (albeit nontrivial) behavior in systems with many strongly-interacting degrees of freedom. These phenomena occur in far-from-equilibrium situations where, due to the intrinsic nonlinear dynamics, and due to the variation of some *control parameter*, a spontaneous breakdown of the spatiotemporal homogeneity leads to either the formation of stationary (space) or rhythmic (time) patterns or to propagating pulses or fronts.

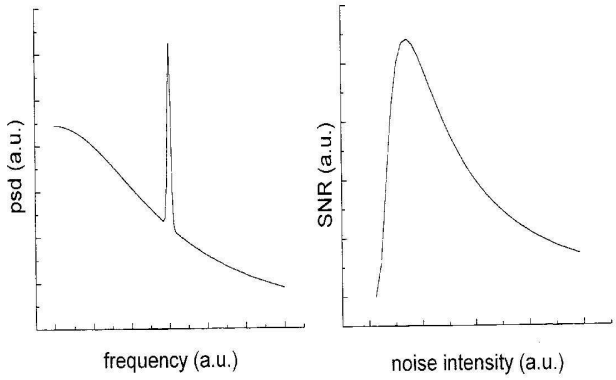

Fig. 7. (i) psd vs. ω and (ii) SNR vs.γ.

There are examples of *dissipative structures* for almost all length scales and in almost all sciences:
(i) mesoscopic: cellular structures in biology, propagation of nerve signals along the neural axon,
(ii) macroscopic: propagation of electric signals in cardiac tissue, pacemakers and spirals in the Belouzov-Zhabotinskii reaction, Bénard convection in fluids, vortex structures in superconductors, social organization in all biological species,
(iii) global and astronomical: convective motion in the ocean, cloud patterns in planetary atmospheres, nebular structures, etc.

Among the many possible descriptions, the *excitable media* picture is one of the most useful ones in the description of pattern formation and propagation. A distributed excitable medium can be viewed as a set of active elements (each element being a system with two or more possible steady states) representing small parts of a continuous system interacting among each other. Typically, such interaction is through some transport mechanism, the most common one being diffusion. It is the interplay between the internal nonlinearities of each element with the coupling among them, together with the effect of external control parameters, that can originate the space-temporal structures.

We will focus our discussion on the *reaction-diffusion model*, studying one- and two-component cases, in order to present some of the underlying principles in pattern formation phenomena.

4.1 Reaction–Diffusion Systems

We will consider a *distributed excitable* medium and assume that the interactions between the different elements that compose the medium are local in time and also that the variation in space is not too sharp, implying that we can neglect memory effects, as well as space derivatives of order higher than

two. Within the formalism discussed in previous sections, the general form of the system equation, for the case of only one relevant macroscopic state variable ϕ, will be

$$\frac{\partial}{\partial t}\phi(\boldsymbol{r},t) \;=\; F(\phi;\nabla\;\phi;\nabla^2\;\phi;\ldots) \tag{84}$$

For the *reaction-diffusion model*, this equation reduces to

$$\frac{\partial}{\partial t}\;\phi(\boldsymbol{r},t) \;=\; F(\phi) \;+\; D\;\nabla^2\;\phi. \tag{85}$$

We will not consider a derivation of this equation, but will adopt it as a phenomenological one. ([63, 14, 23, 15, 51, 58, 53, 82]) For instance, this kind of approach has been found to be adequate for the description of: propagation of electrical signals in cardiac tissue, nervous signals along the neuronal axon, and *target* or *spiral* patterns in the Belousov-Zhabotinskii reaction. ([63, 15, 51, 58, 53])

Clearly, the reaction-diffusion equation for one macroscopic variable shown in (85), can be easily extended to several macroscopic variables $\{\phi_1,\phi_2,..,\phi_n\}$, resulting in a system of coupled reaction-diffusion equations.

However, and in order to proceed with the analysis we will begin by focussing on the one state variable case as in (85), and also initially consider a one dimensional system (i.e.: $\nabla^2 \;\rightarrow\; \partial^2/\partial x^2$).

The first step is to look for stationary solutions, that is to consider $\partial\phi/\partial t \;=\; 0$. Equation (85) reduces to

$$0 \;=\; D\;\frac{\mathrm{d}^2}{\mathrm{d}x^2}\;\phi \;+\; F(\phi). \tag{86}$$

For a one dimensional problem we have seen earlier that the *reaction term* or force $F(\phi)$ can always be derived from a *potential* $V(\phi)$, according to

$$F(\phi) \;=\; \frac{\partial}{\partial\phi}\;V(\phi). \tag{87}$$

In order to fix ideas we resort to an example: the *Schlögl model*, ([23, 51, 53, 82]) that corresponds to the following reaction scheme

$$\begin{aligned} A \;+\; 2\;X &\leftrightarrows 3\;X \\ X &\leftrightarrows B \end{aligned} \tag{88}$$

having the associated macroscopic reaction term

$$F(\phi) \;=\; \kappa_0\;\phi^2 \;-\; \kappa_1\phi^3 \;-\; \kappa_2\;\phi \;+\; \kappa_3, \tag{89}$$

where ϕ is the density of the reactant X, and the constants $\kappa_0,\kappa_1,\kappa_2$ and κ_3 include the reaction rates and the concentration of the reactants A and B. Usually in this model, κ_0 and/or κ_3, are used as control parameters.

Let us consider the bounded domain case: $x \in [-L, L]$, $2L$ being the system length. In principle, we can consider two different boundary conditions
(a) Dirichlet boundary conditions: $\phi(-L) = \phi(L) = 0$, with the physical meaning of perfect absorption on the borders,
(b) Neumann boundary conditions: $\frac{\mathrm{d}}{\mathrm{d}x}\phi(x = -L) = \frac{\mathrm{d}}{\mathrm{d}x}\phi(x = L) = 0$, with the physical meaning of zero flux at the boundary.
Another, more general form of boundary condition, that includes both previous cases as limiting ones, is the *albedo* boundary condition. It describes a situation with partial reflectivity at the boundary. ([72, 82, 26, 27, 28, 85])

We will focus now on the search of inhomogeneous solutions. We write (87) as

$$V(\phi) \; = \; \int_0^{\phi} F(\phi') \; \mathrm{d}\phi', \tag{90}$$

yielding for the Schlögl model the potential ($V(0) = 0$)

$$V(\phi) \; = \; \frac{1}{3} \; \kappa_0 \; \phi^3 \; - \; \frac{1}{4} \; \kappa_1 \phi^4 \; - \; \frac{1}{2} \; \kappa_2 \; \phi^2 \; + \; \kappa_3 \; \phi. \tag{91}$$

The form of equation (86) suggests a mechanical analogy by its interpretation as a particle of mass D, moving under the influence of the potential $V(\phi)$, assimilating the spatial coordinate x to a time variable (varying from $-L$ to L), and ϕ to a spatial coordinate. The first integral of motion yields

$$\frac{D}{2} \left(\; \frac{\mathrm{d}}{\mathrm{d}x} \; \phi \right)^2 \; + \; V(\phi) \; = \; E \; , \tag{92}$$

where E, the analogue of the *total mechanical energy*, is conserved. Exploiting this mechanical analogy, the following features of the solutions of (92) (for the potential given in (91) can be easily seen:
(a) The stationary homogeneous solutions correspond to the extreme of the potential $V(\phi)$.
(b) If we do not impose the Neumann boundary conditions indicated above, then every value of E corresponds to a solution of (86) in the range of $\phi' s$, where $E > V(\phi)$ (for given values of $\phi(-L)$ and $\phi(L)$).
(c) When we impose Neumann boundary conditions, we require that $\phi(-L)$ and $\phi(L)$ became turning points of the *trajectory*, that is $E = V(\phi(-L)) = V(\phi(L))$. This imposes a constraint on the acceptable solutions, restricting them to those confined to the central *valley*. However, such a valley exists only if $\kappa_0 > \kappa_c$ and $\kappa_3 \in [\kappa_{30}, \kappa_{31}]$, where κ_c and κ_{30}, κ_{31} are some extremum values that can be easily determined. ([23, 51, 53, 82]) The other case is a trajectory that starts at the origin ($\phi = 0$), bounces back at some value ϕ^* (with $V(\phi^*) \leq V_{max}$) and returns to the origin.

We can resort to known results from classical mechanics, and see how the possible trajectories in phase space can be parameterized with E, etc. But, due to the lack of space we will not do it here but refer the reader to ([23, 51, 53, 82]).

In general, it is a difficult (if not impossible) task to find explicit solutions either for the stationary problem indicated in (86), or for the (complete) time dependent one in (85). However, there are situations where one is satisfied just with a qualitative analysis of the behavior of such solutions. Clearly then, the study of the stability becomes of primary importance. In this context, the methods developed in previous sections are of relevance.

4.2 Stability for Spatially Extended Systems

In the present case, we linearize the problem about the stationary solution (say $\phi_s(x)$), considering a small time dependent perturbation, and obtain in this way linear differential equations that contain the needed information. Hence, we consider perturbed solutions of the form

$$\phi(x,t) \;=\; \phi_s(x) \;+\; \varphi(x)\; e^{\lambda t} \tag{93}$$

Replacing this into (85), and linearizing in $\varphi(x)$, leads to the following eigenvalue equation

$$D\;\frac{\mathrm{d}^2}{\mathrm{d}x^2}\;\varphi(x) + \left[\frac{\partial}{\partial\phi}\;F(\phi)\right]_{\phi=\phi_s}\varphi(x) \;=\; -\;\lambda\;\varphi(x), \tag{94}$$

whose form, for the case of Neumann boundary conditions, suggests solutions of the type

$$\varphi_n(x) \;\approx\; \cos\left[\frac{n\pi x}{2L}\right], \tag{95}$$

provided that

$$\left(\frac{\partial}{\partial\phi}\;F(\phi)\right)_{\phi=\phi_s} \;-\;\lambda \;=\; D\;\left(\frac{n\pi}{2L}\right)^2. \tag{96}$$

The last equation shows that there is a tight connection between the eigenvalue λ and the wave vector $k = n\pi/2L$ associated to the perturbation. Hence, it is possible to have cases such that, for a certain range of values of the wave length of the perturbation the system is stable, while for other ranges it becomes unstable.

In order to discuss the emergence of an instability, we will consider the scheme from a more general viewpoint, valid for a wide class of systems. Let us start from (85) for a general (infinite) problem, with a stationary homogeneous solution ϕ_s that is stable. The stability of this solution means that our earlier linear stability analysis will give (for a multicomponent system) a set of eigenvalues λ, all having a negative real part (i.e.: $\mathcal{R}e(\lambda) \;<\; 0$). We focus on the one with the largest real part, that we denote by $\lambda(k)$, to make explicit its dependence on the wave vector. Now suppose that there is a control parameter ϵ, whose variation could change the stability of the solution. That is, for $\epsilon < \epsilon_c$ we have $\mathcal{R}e(\lambda(k)) \;<\; 0$ (for all k); while for $\epsilon = \epsilon_c$, $\mathcal{R}e(\lambda(k_0)) > 0$ for some $k = k_0$. Here ϵ_c is the *critical value* of the parameter

ϵ. Usually, for $\epsilon_c \neq 0$, a *reduced* control parameter is used: $\eta = \frac{\epsilon - \epsilon_c}{\epsilon_c}$. We show in Fig.8 the dependence of $\mathcal{R}e(\lambda(k))$ on η. In part (a), for $\eta < 0$, the reference state ϕ_s is stable and $\mathcal{R}e(\lambda) < 0$, but it becomes unstable for $\eta \geq 0$. For $\eta = 0$, the instability sets in, $\mathcal{R}e(\lambda(k_0)) = 0$, at the wave vector $k = k_0$. For $\eta > 0$, there is a band of wave vectors ($k_1 < k < k_2$) for which the uniform state is unstable. For this situation, when $\eta = 0$, we can have two kinds of instabilities: stationary if $\mathcal{I}m(\lambda) = 0$, or oscillatory when $\mathcal{I}m(\lambda) \neq 0$.

If for some reason (usually a conservation law) it happens that $\mathcal{R}e(\lambda(k = 0)) = 0$ for all values of η, another form of instability occurs. It is depicted in part (b) of Fig.8. Here, $k_0 = 0$ is the critical wave vector, and for $\eta > 0$, the unstable band is $0 = k_1 < k < k_2$. It is possible to show that in general $k_2 \approx \eta^{1/2}$, and this indicates that the arising pattern occurs on a long length scale near the threshold $\eta = 0$. Once again we can find steady or oscillatory cases associated with $\mathcal{I}m(\lambda) = 0$ or $\neq 0$.

Finally, in part (c) of the figure, we depict a case where both the instability and the maximum growth rate occur at $k_0 = 0$. This indicates that there is no intrinsic length scale. For this reason the pattern will presumably occur on a scale determined by the system size or by the dynamics. Once again we find steady or oscillatory cases associated with $\mathcal{I}m(\lambda) = 0$ or $\mathcal{I}m(\lambda) \neq 0$. ([7, 59, 8, 82])

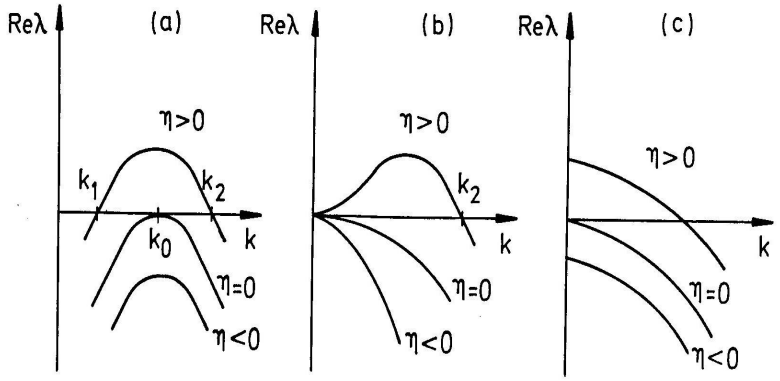

Fig. 8. $\mathcal{R}e(\lambda)$ vs. k.

Another very interesting situation arises, if we have a system of at least two components, when there are two real roots and one of them becomes positive at some critical value of the control parameter. This is a situation leading to a spatially nonuniform steady state that is called a *Turing instability* (at variance with the *Hopf instability* discussed before). ([63, 14, 15, 58])

To close this section it is worth remarking that the kind of analysis we have sketched above leads to the determination of the stability regions for

particular systems. For instance, it allows us to define the so called Büsse or stability balloon, to predict the possible appearance of new instabilities such as the Eckhaus instability (associated with a longitudinal or compressional instability), the zig-zag instability (corresponding to a long-wavelength transversal instability), etc. ([8, 59, 62])

4.3 Examples of Reaction-Diffusion Systems.

Here we will treat two cases of RD models associated to one- and two-component systems. A bistable one-component model corresponding to an electrothermal instability: *the ballast model*; and a two-component model of the *activator-inhibitor* type.

One Component Models: Ballast Resistor.

The most commonly used RD model that exemplifies most of the characteristics we have so far discussed is the *Brusselator*. ([63, 23, 58]) This model, introduced by Prigogine and Lefevre, is a simplified version of more elaborate models showing, qualitatively, a behaviour similar to those observed in experiments related to the *Belousov-Zhabotinskii* reaction, ([63, 23, 15, 51, 58, 53, 82]) and in particular the existence of a transition to a limit cycle. However, we will start here considering a different (one component) model to exemplify the formation of spatial patterns, which is associated with an electrothermal instability: the *ballast resistor*. ([53, 72, 82])

We will adopt a form of the model related to experiments on superconducting microbridges, called the *hot-spot* model. ([74]) We consider a thin wire of a superconductor metal of length $2L$, along which an electric current I is flowing. The wire is immersed in a heat bath with constant temperature T_B. Depending on the values of these parameters, the temperature profile on the wire will be either homogeneous, or inhomogeneous (regions with different temperatures coexisting along the wire). The law of conservation of internal energy per unit length of the wire $u(x,t)$ can be writing as

$$\frac{\partial}{\partial t}\, u(x,t) \;=\; -\;\frac{\partial}{\partial x}\;\left(J(x,t)\;+\;h(x,t)\;I(x,t)\right)\;-\;Q(x,t)\;+\;I(x,t)E(x,t), \tag{97}$$

where x is the position along the wire ($-L \le x \le L$), J is the heat current, h is the enthalpy per unit of charge carrier and unit length, Q is the energy flow dissipated into the gas per unit length, E is the electric field along the wire and IE is the heat generated by the current per unit length. As the Coulomb forces between the charges are very strong, we assume electro-neutrality of the wire, yielding $\frac{\partial}{\partial x}\; I(x,t) \;=\; 0 \quad \Leftrightarrow \quad I(x,t) \;=\; I(t)$. However, this assumption will only be valid if one considers a range of time variation that is short when compared with the inverse of the typical plasma frequency of the electrons.

Using the fact that the quantities J, E and Q obey some phenomenological linear laws, as well as Onsager relations between different "transport coefficients" (Peltier and Thompson coefficients, etc), together with the relation between the internal energy of the wire $u(x,t)$ and the local temperature field $T(x,t)$ ($\mathrm{d}u(x,t) = c\ \mathrm{d}T(x,t)$, with c the heat capacity per unit length) we obtain the system's equation for the temperature profile on the wire ([72, 82])

$$c\ \frac{\partial}{\partial t}\ T(x,t)\ =\ \frac{\partial}{\partial x}\ \lambda\ \frac{\partial}{\partial x}\ T\ -\ q\ (T\ -\ T_B)\ +\ R\ I^2. \tag{98}$$

Here λ is the heat conductivity of the wire, R the isothermal resistivity per unit length, and q is related to the energy dissipated into the gas due to the difference in temperature between the wire and the gas. All these coefficients may, in principle, depend on the local temperature of the wire, while q may also depend on T_B. In order to further simplify the equation for the temperature profile, we assume that the specific heat c, the heat conductivity λ and the heat transfer coefficient q are all constant along the wire.

As discussed earlier, we are interested in stationary solutions for the temperature field distribution. Hence, our equation has the form

$$0\ =\ \lambda\ \frac{\mathrm{d}^2}{\mathrm{d}x^2}\ T\ -\ q\ (T\ -\ T_B)\ +\ R\ I^2. \tag{99}$$

For the resistivity R we will adopt a piecewise-linear approximation of a realistic one (see the l.h.s. of Fig.9), according to $R(T)\ =\ R_o\ \theta[T(x,t)\ -\ T_c]$, (with $\theta(z)$ the step function: $\theta(z) = 1$ for $z > 0, \theta(z) = 0$ for $z < 0$)). The assumption behind of such a form is that for $T < T_c$ the wire is superconducting while it has a finite (constant) resistivity for $T > T_c$. Without loss of generality we take the zero of the temperature scale at the heat bath temperature T_B ($T_B = 0$). We also make a scaling of the parameters in order to have nondimensional coordinates ($y \equiv (q/\lambda)^2 x$, and $y_L = (q/\lambda)^2 L$, with $-y_L \le y \le y_L$). In our discusion we will assume that the current I is fixed (the voltage difference depending on I), and we define the following "effective temperature"

$$T_h\ \equiv\ I^2 R_o/q$$

With all these assumptions, equation (99) for T adopts the final form

$$\frac{\mathrm{d}^2}{\mathrm{d}y^2}\ T(y)\ -T\ +\ T_h\ \theta[T(x,t)\ -\ T_c]\ =\frac{\mathrm{d}^2}{\mathrm{d}y^2}\ T(y)\ +\ \frac{\mathrm{d}}{\mathrm{d}T}\ V[T]\ =\ 0 \tag{100}$$

where the potential $V(T)$ is defined according to (91) as

$$V(T)\ =\ \int_0^T \mathrm{d}T'\ \left(T_h\theta[T' - T_c]\ - T'\right). \tag{101}$$

The shape of the function $F(T) = \frac{\partial}{\partial T} V(T)$, as well as the approximation adopted for the resistivity, are shown in Fig.9.

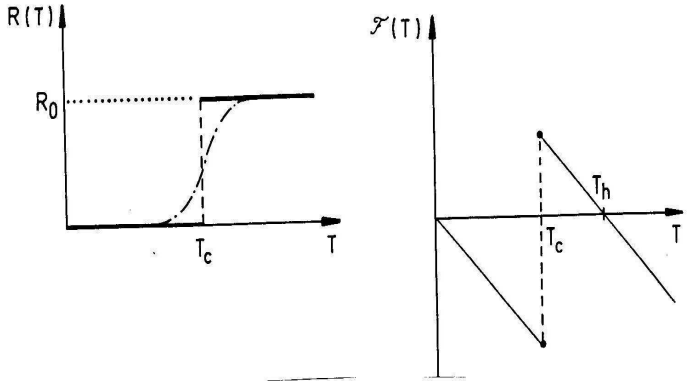

Fig. 9. Approximate forms of $R(T)$ and $F(T)$ for the ballast model.

When we compare the present form of the nonlinear function $F(T)$ with the corresponding term in the Schlögl model of equation (91), we see that the ballast model *mimics* the Schlögl model.

To complete the model, we need to specify the boundary conditions at both borders: $x = \pm L$ (or $y = \pm y_l$). As commented above, we will only consider Dirichlet or Neumann boundary conditions.

To find the form of the stationary solutions one may distinguish two different regions

(i) *Cold regions*, where $T(y) < T_c$, and (100) reduces to

$$\frac{\mathrm{d}^2}{\mathrm{d}y^2} T(y) - T = 0, \tag{102}$$

with solutions that have the general form $T(y) = A_c \mathrm{e}^{y} + B_c \mathrm{e}^{-y}$;

(ii) *Hot regions*, where $T(y) > T_c$, and (100) reduces to

$$\frac{\mathrm{d}^2}{\mathrm{d}y^2} T(y) - T + T_h = 0, \tag{103}$$

and with general solutions of the form $T(y) = A_h \mathrm{e}^{y} + B_h \mathrm{e}^{-y} + T_h$

The parameters A_c, B_c, A_h and B_h are determined after imposing the boundary conditions. Furthermore, if we have a cold region on the left and a hot region on the right of a certain position coordinate y_c (or vice versa), both solutions should be joined together in such a way that (100) is satisfied at the transition point. This is the case if both T and $\mathrm{d}T/\mathrm{d}y$ are continuous at $y = y_c$. Using these conditions, it is clear that

$$T(y_c) = T_c$$

allowing us to fix the value of y_c.

Let us now analyze the stationary states. We first consider the homogeneous case. For Neumann B.C. the potential $V(T)$ must have a maximum.

This leads to $T(y) = 0$ for all values of T_h (and therefore of the current I). However, if $T_h > T_c$, there is an additional homogeneous solution $T(y) = T_h$. Clearly both satisfy the Neumann boundary conditions. For Dirichlet B.C., there is only one possible homogeneous solution $T(y) = 0$.

We now turn to inhomogeneous stationary temperature profiles. Using the mechanical analogy, it is possible to find inhomogeneous solutions corresponding to several *rebounds* between the *turning points* of the potential. But here we will consider spatial temperature distributions having only one maximum, with two *cold* regions for $-y_L < y < -y_c$ and $y_c < y < y_L$, and one *hot* region for $-y_c < y < y_c$ (with two transition points at $y = \pm y_c$ due to symmetry). Through a linear stability analysis one may prove that solutions with several maxima are always unstable.

Imposing the boundary conditions (Neumann or Dirichlet) on the solutions of the form indicated above, the different constants are determined yielding the typical shapes indicated in Fig.10; part (a) for Dirichlet and (b) for Neumann b.c.

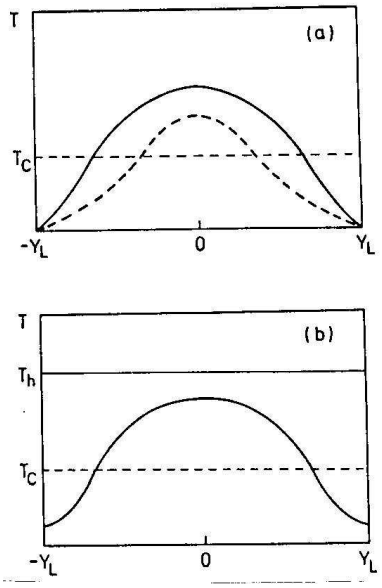

Fig. 10. Patterns in the ballst model: (a) Dirichlet b.c., (b) Neumann b.c.

According to linear stability analysis we can conclude that, for Dirichlet b.c., from the pair of simultaneous solutions, the one with the larger dissipation (i.e. the larger hot region) is stable while the other is unstable. Similarly, for the case of Neumann b.c., indicates that the homogeneous stationary solutions are stable, while inhomogeneous structures are always unstable.

Now, we will briefly discuss how to describe the propagation of structures in one component systems, considering (86) once more in its complete form.

We assume a one dimensional, infinite, system. To complete the description, we need to include some boundary conditions at infinity. Clearly, for a very general form of $F(\phi)$ it is not easy to find an arbitrary solution of (86) fulfilling the chosen b.c. However, there is a particular kind of solutions of great interest called *solitary waves* on which we will now focus our attention. These waves are functions of the spatial (x) and temporal (t) coordinates, not independently, but through the combination $\xi = x - ct$. In terms of the new variable ξ, (86) adopts the form

$$D \frac{\partial^2}{\partial \xi^2} \phi + c \frac{\partial}{\partial \xi} \phi + F(\phi) = 0. \tag{104}$$

where $\frac{\partial}{\partial t} = -c \frac{\partial}{\partial \xi}$ and $\frac{\partial^2}{\partial x^2} = \frac{\partial^2}{\partial \xi^2}$.

Here we can resort once more to the mechanical analogy used earlier (see Sect.4.1). We again interpret ϕ as the spatial coordinate of a particle of mass D moving in the force field $F(\phi)$ (derived from the potential $V(\phi)$, i.e. $F(\phi) = \frac{\partial V}{\partial \phi}$), but now in the presence of a *friction force* proportional to the velocity of the particle, i.e. $\frac{\partial \phi}{\partial \xi}$. Hence, c plays the role of the friction coefficient.

Let us concentrate on the situation where the potential $V(\phi)$ has a bistable form, and ask for solutions of (104) with the boundary conditions

$$\phi \to \phi_2 \quad \text{for} \quad \xi \to -\infty$$
$$\phi \to \phi_1 \quad \text{for} \quad \xi \to \infty$$

with ϕ_1 and ϕ_2 the stationary solutions. The resulting wave, or moving pattern, is called a *trigger* or *front wave*, because its propagation triggers the transition from one stationary state of the system to the other (both minima of V). This kind of waves has been observed, for instance, in chemically reacting media or as electrical activity that propagates without attenuation along the axonal membrane.

In order to analyze qualitatively the behavior of a bistable system, for instance the dependence of the (unique) front velocity on the potential parameters, we can exploit again the form of the ballast resistor model introduced before. However, and always due to the lack of space, we refer to ([58, 53, 72, 82, 26, 27, 28, 5]).

We now turn to discuss the propagation phenomenon in systems with two components.

Many Component Models: Activator–Inhibitor

In order to make a realistic description, for the theoretical representation of travelling waves of chemical, physical or biological activity commonly observed in spatially distributed excitable media, we need to resort to models

with more than one component. All excitable media share certain characteristic features. They have a stable rest state, and small perturbations are rapidly damped out. However, perturbations larger than a certain threshold trigger an abrupt and substantial response. After this fast response, the media is typically refractory to further stimulation for some characteristic time before it recovers its full excitability. It is clear that such a sequence of events cannot be represented by a simple one component model of the kind we have discussed so far. On the other hand, the analysis of a model with a large number of components quickly becomes too cumbersome. Notwithstanding, experience has shown that it is enough to resort to two component models in order to be able to qualitatively (and sometimes quantitatively) reproduce several characteristics of real systems. ([14, 15, 58, 53, 82])

The set of equations corresponding to a model describing a two component system, with densities $u(x,t)$ and $v(x,t)$, according to (85), ([14, 15, 58, 53, 82]) has the general form

$$\begin{aligned} \frac{\partial}{\partial t}\, u(x,t) &= D_u\, \frac{\partial^2}{\partial x^2}\, u \;+\; f(u,v) \\ \frac{\partial}{\partial t}\, v(x,t) &= D_v\, \frac{\partial^2}{\partial x^2}\, v \;+\; g(u,v) \end{aligned} \tag{105}$$

Depending on the actual form of the nonlinear terms $f(u,v)$ and $g(u,v)$, even such an innocent looking pair of equations, can have an extremely complicated behavior. However, the experience has also shown that a typical and very fruitful form is the one shown in Fig.11. There, we show in the phase plane (u,v), the form of the nullclines (that is the curves $f(u,v) = 0$ and $g(u,v) = 0$), and the sign of the derivatives of the nonlinear reactive functions in each plane region.

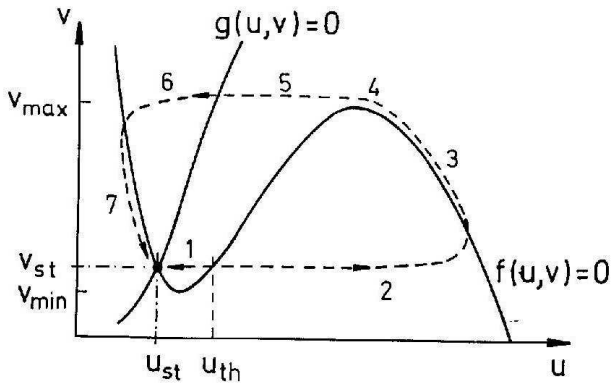

Fig. 11. Nullclines of the activator-inhibitor systems.

We will now qualitatively discuss how it is that such a simple system can model the sequence of events we have indicated at the beginning of this section. We recall that an excitable medium is a spatially distributed system composed of excitable elements. The interaction between neighboring elements through a diffusive coupling makes it possible to produce excitation waves. If a local region of space is disturbed beyond a certain threshold value, then the autocatalytic production of substance u within the excited region causes u to diffuse into the neighboring regions, driving those regions across the threshold and thus making the excitation spread spatially. This corresponds to a front propagation. In order to make a pictorial representation of this process, we refer to Fig.11. There is a unique homogeneous steady state indicated by the point (u_{st}, v_{st}), that satisfies $f(u_{st}, v_{st}) = 0$ and $g(u_{st}, v_{st}) = 0$, and is locally stable but excitable: while the subthreshold disturbances are rapidly damped (perturbations in the region indicated by 1 in Fig.11), larger disturbances (those driving the system beyond the point u_{th}) provoke an excitation cycle that is governed by the local reaction kinetics before the system returns to the steady state. This cycle is indicated in the figure through the sequence of numbers from 2 to 7, corresponding to different states of the system. In region 2, u increases by an autocatalytic process, until the phase trajectory reaches the curve $f(u, v) = 0$, where the density of v starts to increase, and the process evolves following the nullcline as indicated by 3. After that the process reaches a maximum value of the density for v in 4, and follows curve 5, where the density of u decreases and after crossing the nullcline $g = 0$, region 6, the other branch of the nullcline $f = 0$ is reached and the system moves along this trajectory (indicated by 7) and reaches the steady state (u_{st}, v_{st}) again.

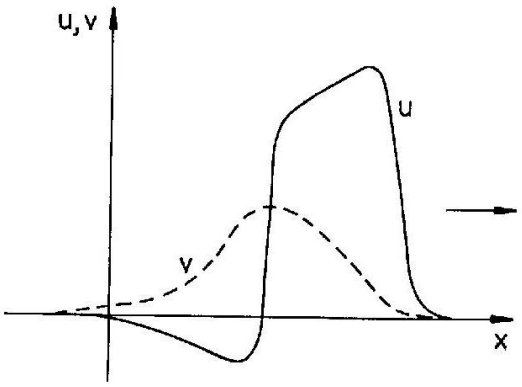

Fig. 12. Activator and inhibitor profiles.

We have seen that the abrupt over-threshold autocatalytic production of u gives rise to the excitability of the system and the interaction between

u and v causes the recovery from the excitation state. For this reason the variable u is sometimes called the *trigger* variable and v the *recovery* variable (or *propagator* and *inhibitor*, respectively). For instance, some examples in real systems are: membrane potential as *propagator* and ionic conductance as *inhibitor* in neuromuscular tissue; bromous acid as *propagator* and ferroin as *inhibitor* in the Belousov-Zhabotinskii reaction; infectious agent as *propagator* and level inmunity as *inhibitor* in epidemics.

A typical form of the profile in a one dimensional media for the kind of waves that behave according to the previous description is shown in Fig.12. The transition zone from the resting to the excited state is called the *front*, while the transition zone from the excited to the resting state is the *backfront*.

The process we have so far discussed is clearly not restricted to a one dimensional geometry. In fact, in two dimensional media the same line of argument leads to describing the so called *target structures*, that is perturbations that spread radially originating a sequence of growing rings, such as has been observed in the Belousov-Zhabotinskii reaction. When we look at such structures far from the point where they originated, the curvature has decreased and the structure acquires a one dimensional characteristic, i.e. in the direction of propagation it has the same profile as shown in Fig.12, while it extends "infinitely" in the normal direction.

Let us now qualitatively discuss the origin of a very important type of structure that arises in (two dimensional) *propagator-inhibitor* systems: the *spirals*.

Spirals in propagator-inhibitor systems

A common form of pattern in the reaction-diffusion description of two-dimensional excitable media is the rotating *spiral*. The interest in this kind of pattern is due to its occurrence in chemical (i.e. the Belouzov-Zhabotinskii) reactions as well as in biological systems (waves of electrical and neuromuscular activity in cardiac tissue, formation of some bacterial colonies). A complete mathematical description of such structures is extremely difficult. However, within the *propagator-inhibitor* scheme, it is possible to understand intuitively the initial stage in the formation of an spiral wave. ([15, 58, 53, 82]) We start considering a thought experiment in a two dimensional medium with a one dimensional solitary wave of the type discussed earlier. That means a propagating straight band, a two-dimensional wave with a profile in the direction of motion like the one shown in Fig.12, and extending indefinitely in the normal direction. Assume that such a band is perturbed in some way (for instance by a light beam incident on a photosensitive reactant). Hence, the pulse-like structure is disturbed in that region, taking the form indicated on the r.h.s. of Fig.13. It is clear that in both branches of the perturbed structure we will see that the points in the front or in the backfront will continue their motion. The only exception will be the point indicated by v^* (that will correspond to the *tip* of the *spiral core*). This point is the boundary between

the front and the backfront and, if we consider that the front velocity has to change continuously, it must have zero velocity.

The evolution will develop according to the following steps. We refer our argumentation to Fig.13. On the left, we depict the upper branch of the perturbed band. The points on the front, far from v^*, move at the same original velocity, but when we come closer to v^*, their velocity reduces continuously. The same happens with points on the backfront. This initial situation is indicated by the curve labelled a . After a short time has elapsed, the point v^* remains immobile, but all other points have moved into their new positions indicated by the curve labelled b. Clearly, the original form of the perturbed band is deformed. After another short time elapses, the same process is repeated and the curve changes to the one labelled c; after another short time to d, and so on. Carried to its logical extreme, this type of analysis would predict that the front would acquire a growing angular velocity and curvature, a process that finally produces a spiral.

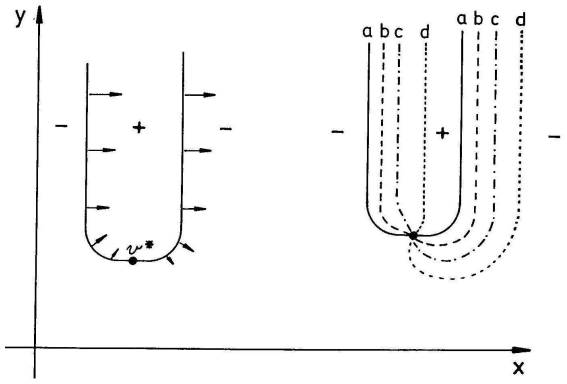

Fig. 13. The genesis of spirals.

The experimental observation of spirals in chemically reactive media, particularly in the Belouzov-Zhabotinskii reaction, shows that this kind of pattern appears as pairs of symmetric, counter-rotating spirals. To understand this aspect within the same qualitative picture we must remember that originally there were two branches. However, each one is the specular image of the other, implying that, if the motion in the neighborhood of the upper one is a rotation in the indicated direction, the motion around the one on the bottom will be a rotation in the opposite direction. Hence, the same picture offers a description on the possible origin of spirals as well as their appearance in counter-rotating pairs.

5 Nonequilibrium Potential

Let us now go back to the dynamical system (1) and discuss the *effect of noise*. ([19, 20, 21]) We start writing

$$\frac{\mathrm{d}x_j}{\mathrm{d}t} = F_j(\boldsymbol{x}) \; + \; \sum_l \; \boldsymbol{g}_{jl}\xi_l(t), \tag{106}$$

where $\xi_l(t)$ are white noise terms of zero mean and correlations $\langle \xi_j(t)\xi_l(t')\rangle = 2\;\gamma\;\delta_{jl}\;\delta\;(t-t')$. The associated FPE for $P((\boldsymbol{x}),t) \;=\; P(x_1,\ldots,x_n,t)$, will be a generalization of (64) given by

$$\frac{\partial}{\partial t}P(\boldsymbol{x},t) = \sum_j \frac{\partial}{\partial x_j}\left(-[F_j(\boldsymbol{x})\;P(\boldsymbol{x},t)] + \gamma \sum_l \frac{\partial}{\partial x_l}[\boldsymbol{G}_{jl}\;P(\boldsymbol{x},t)]\right) \tag{107}$$

with $\boldsymbol{G} \;=\; \boldsymbol{g}\boldsymbol{g}^T$. If we can write that $F_j(\boldsymbol{x}) \;=\; \sum_l(\$)_{jl}\frac{\partial}{\partial x_l}V(\boldsymbol{x})$, we find again the situation studied in Sect.**2.4** where, from a deterministic point of view, we have a *relaxational flow*. Hence, if $\boldsymbol{G} \;=\; \$$, it is possible to derive the expression

$$P_{st}(\boldsymbol{x}) \simeq \mathrm{e}^{-V(\boldsymbol{x})/\gamma}. \tag{108}$$

Clearly, if $g_{jl} \;=\; \delta_{jl}$, the result is trivial.

Let us now consider the case where $F_j(\boldsymbol{x}) \;=\; -\sum_l(\$)_{jl}\frac{\partial V}{\partial x_l} \;+\; w_j$, that in analogy with Sect.**2.4** corresponds to a *nonrelaxational flow*. We assume that $\$ = \boldsymbol{g}.\boldsymbol{g}^T$. Hence we will have that the Hamilton–Jacobi like equation (26) that now reads

$$\sum_l \left(F_l \;+\; \sum_j(\$)_{jl}\frac{\partial V}{\partial x_j}\right)\;\frac{\partial V}{\partial x_l} \;=\; 0, \tag{109}$$

yields, in the deterministic case, a function $V(\boldsymbol{x})$ that is a Lyapunov functional of the problem. However, it has been proved by Graham and collaborators ([19, 20, 21]) that in such a case and in the weak noise limit ($\gamma \to 0$), the stationary solution of the multivariate FPE (107) associated to the set of SDE (106) is given by

$$P_{st}(\boldsymbol{x}) \sim \mathrm{e}^{-V(\boldsymbol{x})/\gamma + O(\gamma)}. \tag{110}$$

with $V(\boldsymbol{x})$ the solution of (109). This functional corresponds to the *nonequilibrium* or *Graham's potential*. ([19, 20, 21])

As discussed in the introduction, we can interpret the effect of noise saying that it induces fluctuations in the system around one of the minima of $V(\boldsymbol{x})$, fluctuations that allow the system to explore the neighborhood of such a point and in this way identify it as a minimum.

The knowledge of the potential $V(\boldsymbol{x})$ offers us, at least in principle, the possibility of getting information about

1. fixed points (extrema of $V(\boldsymbol{x})$),
2. local stability of the fixed points,
3. global stability of the minima (attractors),
4. barrier heights between different minima,
5. decay times of metastable states.

It is the last point, decay of metastable states, one of the aspects that will be discussed in the following subsections.

5.1 Some Examples of Nonequilibrium Potentials in RD Systems

In relation with pattern formation, boundary conditions (b.c.) have been recently shown to play a relevant role in the appearance and stability as well as on the propagation of spatial structures, for one and two–component systems. ([72, 85, 26, 27]) More recently, the role of b.c. in pattern selection, and more particularly the *global stability* of the resulting structures have been analyzed. ([33, 34, 35]) Such analysis was carried out by exploiting the notion of *nonequilibrium potential* or *Lyapunov functional* (LF) of the system. This kind of approach has not been used in the realm of RD systems because it is usually not possible, insofar as some potential conditions are not fulfilled, to obtain a Lyapunov function for a general problem. However, the results of Graham and collaborators ([19, 20, 21]) point to the possibility of getting information about such functionals as well as about global stability even though the system does not fulfill the above indicated potential conditions.

When the LF exists, such an approach offers an alternative way of confronting a problem that has recently attracted considerably attention, both experimentally and theoretically. Namely, the relative stability of the different attractors, corresponding to spatially extended states, and the possibility of transitions among them due to the effect of (thermal) fluctuations. ([40, 75, 77, 29, 55])

In this section we will show the results on local and global stability, obtained by means of the nonequilibrium potential, through a couple of simple examples.

Ballast Resistor.

The specific model we shall focus on in this section, with a known form of the LF or nonequilibrium potential, corresponds to the same simple one–dimensional, one–component model of an electrothermal instability discussed in Sect.4.3. However, it can be considered as mimicking a broader class of bistable reaction–diffusion models. The particular, nondimensional form that we shall work with is

$$\partial_t T = \partial^2_{yy} T - T + T_h \theta(T - T_c). \tag{111}$$

In ([33]), both the global stability of the patterns and the relative change in stability for this model were analyzed, as some b.c. parameter was changed. Here we analyze how those results depend on the threshold parameter.

For the sake of concreteness, we consider here a class of stationary structures $T(y)$ in the bounded domain $y \in (-y_L, y_L)$ with Dirichlet boundary conditions at both ends, $T(y = \pm y_L) = 0$. These are the spatially symmetric solutions to (111) already discussed in Sect.4.3. Such structures can also be seen as a symmetrization of a set of stationary solutions to the Ballast reaction-diffusion model in the interval $(0, y_L)$ with a Neumann boundary condition at $y = 0$, namely, $dT/dy|_{y=0} = 0$.

The explicit forms of the stationary structures are

$$T(y) = T_h \times \begin{cases} \sinh(y_c)\sinh(y_L + y)/\cosh(y_L), & -y_L \le y \le -y_c, \\ 1 - \cosh(y)\cosh(y_L - y_c)/\cosh(y_L), & -y_c \le y \le y_c, \\ \sinh(y_c)\sinh(y_L - y)/\cosh(y_L), & y_c \le y \le y_L, \end{cases} \tag{112}$$

The double-valued coordinate y_c, at which $T = T_c$, is given by

$$y_c^{\pm} = \frac{1}{2} y_L - \frac{1}{2} \ln \left[z \cosh(y_L) \pm \sqrt{z^2 \cosh(y_L)^2 - 1} \right], \tag{113}$$

with $z = 1 - 2T_c/T_h$ $(-1 < z < 1)$.

When $y_c^{\pm}$ exists and $y_c^{\pm} < y_L$, the solution (112) represents a structure with a central hot zone $(T > T_c)$ and two lateral cold regions $(T < T_c)$. For each parameter set there are two stationary solutions, given by the two values of y_c. In ([72]), it has been shown that the structure with the smallest hot region is unstable, whereas the other one is linearly stable. The trivial homogeneous solution $T = 0$ exists for any parameter set and is always linearly stable. These two linearly stable solutions are the only stable stationary structures under the chosen boundary conditions. Therefore, under suitable conditions, we have a bistable situation in which two stable solutions coexist, one of them corresponding to a cold–hot–cold (CHC) structure and the other one to the homogeneous trivial state. The unstable solution is always a CHC structure, with a relatively small hot region.

For the symmetric solution we are considering here, the nonequilibrium potential or LF reads ([33])

$$\mathcal{F}[T] = 2 \int_0^{y_L} \left\{ - \left(\int_0^T \left[-T' + T_h \theta(T' - T_c) \right] \mathrm{d}T' \right) + \frac{1}{2} (\partial_y T)^2 \right\} \mathrm{d}y. \tag{114}$$

Replacing (112), we obtain the explicit expression

$$\mathcal{F}^{\pm} = -T_h^2 y_c^{\pm} z + T_h^2 \sinh(y_c^{\pm}) \frac{\cosh(y_L - y_c^{\pm})}{\cosh(y_L)}. \tag{115}$$

For the homogeneous trivial solution $T(y) = 0$, instead, we have $\mathcal{F} = 0$.

In Fig.14 we have plotted the LF $\mathcal{F}[T]$ as a function of $\phi_c = T_c/T_h$ for a fixed system size. The curves correspond to the inhomogeneous structures, $\mathcal{F}^{\pm}$, whereas the horizontal line stands for the LF of the trivial solution. The upper branch of each curve is the LF of the unstable structure, where $\mathcal{F}$ attains a maximum. At the lower branch and for $T = 0$, the LF has a local minimum. The curve exists up to a certain critical value of ϕ_c at which both branches collapse. The critical behavior, around this point (which we will not discuss here) was analyzed in ([86, 5]).

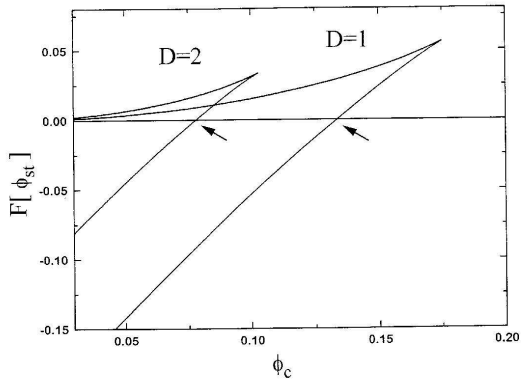

Fig. 14. Nonequilibrium potential $\mathcal{F}$, for the stationary patterns of the ballast resistor, as a function of ϕ_c, for $L = 1$. The bottom curve corresponds to $\phi_s(y)$ and the top one to $\phi_u(y)$. The points ϕ_c^*, are indicated.

It is interesting to note that, since the LF for the unstable solution is always positive and, for the stable CHC structure, $\mathcal{F} < 0$ for $\phi_c \to 0$, and > 0 otherwise, the LF for this structure vanishes for an intermediate value of the parameter: $\phi_c = \phi_c^*$. At that point, the stable inhomogeneous structure and the trivial homogeneous solution interchange their relative stability. In fact, $T(y) = 0$ switches from being a metastable state, to being more stable than the inhomogeneous structure.

Activator–Inhibitor.

The importance of activator-inhibitor systems for applications in physics, chemistry and biology is by now very well established. ([42, 44, 64, 65, 66, 85, 67, 18, 12]) Here we shall focus on a specific system belonging to this family of two–component models. We want to present an analysis of the global stability of stationary patterns exploiting the concept of nonequilibrium potential.

We start with a simplified (piecewise linear) version of the activator–inhibitor model sketched in Sect.4.3, which preserves the essential features, and fix the parameters so as to allow for nontrivial solutions to exist. After

scaling the fields, we get a dimensionless version of the model as:

$$\begin{aligned} \partial_t u(x,t) &= D_u \partial_x^2 u - u + \theta[u-a] - v \\ \partial_t v(x,t) &= D_v \partial_x^2 v + \beta u - \gamma v \end{aligned} \tag{116}$$

We confine the system to the interval $-L < x < L$ and impose Dirichlet boundary conditions on both extrema. According to the values of the parameters a, β and γ, we can have a monostable or a bistable situation. ([42, 65]) In the second case we have two homogeneous stationary (stable) solutions. One corresponds, in the (u, v) plane, to the point $(0, 0)$ while the other is given by (u_0, v_0) with

$$u_0 = \frac{\gamma}{\beta+\gamma} \ , \ v_0 = \frac{\beta}{\beta+\gamma}$$

implying that the condition $\frac{\gamma}{\beta+\gamma} > a$ must be fulfilled. Without losing generality we may assume that $0 < a < 1/2$ and $u_0 < 2a$. ([42])

The inhomogeneous stationary patterns appear due to the nonlinearity of the system, and ought to have activated regions ($u > a$) coexisting with non-activated regions ($u < a$). This fact, together with the symmetry of the evolution equations and boundary conditions, implies the existence of symmetric inhomogeneous stationary solutions. We restrict ourselves to the simplest inhomogeneous, symmetric, stationary solutions. That is, a symmetric pattern consisting of a central region where the activator field is above a certain threshold ($u > a$) and two lateral regions where it is below it ($u < a$). As was already discussed, ([42, 85], different analytical forms (which are here linear combinations of hyperbolic functions) should be proposed for u and v depending on whether $u > a$ or $u < a$. These forms, as well as their first derivatives, need to be matched at the spatial location of the transition point, which we called x_c. Through that matching procedure and imposing boundary conditions we get the general solution for the stationary case. In order to identify the matching point x_c we have to solve the equation $u(x_c) = a$, resulting in general in a transcendental equation for x_c. In order to avoid the complications arising from the possible spatially oscillatory behavior of the solutions, we will work in a parameter range where the diffusion coefficient of the activator (D_u) is lower than some critical value (D_u^{osc}), [42, 65], beyond which the solutions became spatially oscillatory. In particular there are up to four different solutions for x_c, and associated with each one we have different stationary solutions that we will indicate by u_{e1}, u_{e2}, u_{e3} and u_{e4}, with increasing values of the transition point x_c. A linear stability analysis of these solutions indicates that u_{e1} and u_{e3} are unstable while u_{e2} and u_{e4} are locally stable. The stable states will correspond to attractors (minima) of the functional while the unstable ones will be saddle points, defining the barrier height between attractors.

We now write the equations of our system specifying the time scale associated with each field. This allows us to perform an adiabatic approximation

and obtain a particular form of the nonequilibrium potential for this system. Measuring the time variable on the characteristic time scale of the slow variable u (i.e.: τ_u), (116) adopt the form

$$\begin{aligned} \partial_t u(x,t) &= D_u \partial_x^2 u(x,t) - u(x,t) + \Theta[u(x,t)-a] - v(x,t) \\ \eta\ \partial_t v(x,t) &= D_v \partial_x^2 v(x,t) + \beta u(x,t) - \gamma v(x,t) \end{aligned} \tag{117}$$

where $\eta = \tau_v/\tau_u$. At this point we assume that the inhibitor is much faster than the activator (i.e.: $\tau_v \ll \tau_u$). In the limit $\eta \to 0$, we can rewrite (117) as

$$\begin{aligned} \partial_t u(x,t) &= D_u \partial_x^2 u(x,t) - u(x,t) + \Theta[u(x,t)-a] - v(x,t) \\ 0 &= D_v \partial_x^2 v(x,t) + \beta u(x,t) - \gamma v(x,t) \end{aligned} \tag{118}$$

In the last pair of equations we can eliminate the inhibitor (now *slaved* to the activator) by solving the second equation using the Green function method

$$\begin{aligned} \{-D_v \partial_x^2 + \gamma\} G(x,x') &= \delta(x-x') \\ v(x) &= \beta \int dx' G(x,x') u(x'). \end{aligned} \tag{119}$$

This slaving procedure reduces our system to a *nonlocal* equation for the activator only, having the form

$$\partial_t u(x,t) = D_u \partial_x^2 u(x,t) - u(x,t) + \Theta[u(x,t)-a] - \beta \int dx' G(x,x') u(x') \tag{120}$$

From this equation, and taking into account the symmetry of the Green function $G(x,x')$, we can obtain the Lyapunov functional for this system, which has the form

$$\begin{aligned} \partial_t u(x,t) &= -\frac{\delta \mathcal{F}[u]}{\delta u} \\ \mathcal{F}[u] &= \int dx \left\{ \frac{D_u}{2} \left\{\partial_x u\right\}^2 + \frac{u^2}{2} - (u-a)\Theta[u-a] \right. \\ &\qquad \left. + \frac{\beta}{2} \int dx' G(x,x') u(x') u(x) \right\} \end{aligned} \tag{121}$$

The spatial nonlocal term in the nonequilibrium potential takes into account the repulsion between activated zones. When two activated zones come near each other, the exponential tails of the inhibitor concentration overlap, increasing its concentration between both activated zones and creating an *effective* repulsion between them, the Green function playing the role of an exponential screening between the activated zones.

We can now exploit this LF in order to discuss the stability of the stationary solutions found earlier. According to the analysis done in ([12]), we can see that, obtaining the "curvature" of the potential is equivalent to diagonalizing the operator $\mathcal{F}_2[u_e]$ and finding its eigenvalues. Such an analysis is completely analogous to the linear stability one.

A very interesting point is to analyze the stability of the stationary solutions just found, as functions of the activator diffusivity. In Fig.15 we show the dependence of the LF vs. D_u for the different patterns. We see that this dependence of the LF for the different patterns; u_{e1} through u_{e4}, is compatible with the results of a linear stability analysis. A more complete analysis of this problem can be found in ([12]).

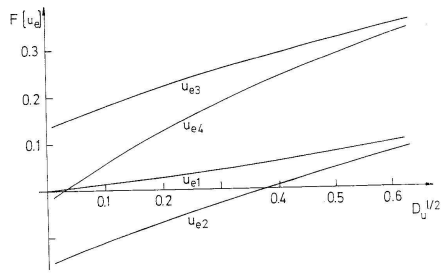

Fig. 15. Nonequilibrium potential as a function of D_u for the activator-inhibitor system with fast inhibitor. The potential for the different stationary states are indicated by its label u_{ei}, $i = 1 - 4$.

5.2 Stochastic Analysis

We study here the decay of a metastable rest state under the action of external noise. The noise strength is assumed to be weak enough, assuring us that the stability of the patterns without noise is qualitatively not altered. We have previously found that there are locally stable uniform and non–uniform steady states and an unstable non–uniform state with a critical radius, which is a saddle point in the functional space. To obtain the transition probability between metastable and stable states, it is necessary to find the conditional probability for the random field $\phi(\boldsymbol{r}, t)$ to be in the stable state $\phi_{stable}(\boldsymbol{r}, t)$ at time t, given that at the initial time $t = 0$ the system was in a metastable state $\phi_{meta}(\boldsymbol{r}, 0)$. This probability can be represented by a path integral ([73, 46, 81]) over those realizations of the random field $\xi(\boldsymbol{r}, t)$ that satisfy the initial and final conditions, that is:

$$P[\phi_{stable}(\boldsymbol{r}, t)|\phi_{meta}(\boldsymbol{r}, 0)] \sim \int Q[\xi]\, \delta[\phi(\boldsymbol{r}, t) - \phi_{meta}(\boldsymbol{r}, 0)]\, \mathcal{D}\xi(\boldsymbol{r}, t), \quad (122)$$

where the statistical weight $Q[\xi]$ for a Gaussian white noise is:

$$Q[\xi] = \mathcal{M}\, \mathrm{e}^{-\frac{1}{2\gamma}\int_0^t \mathrm{d}t \int \mathrm{d}r\ \xi^2(\boldsymbol{r},t)}, \tag{123}$$

where $\mathcal{M}$ is a normalization constant. In the limit of small noise intensity ($\gamma \to 0$), the main contribution in (122) comes from those realizations of the field in the neighborhood of the most probable trajectory. Under this conditions, (122) can be estimated by the steepest–descent method.

Due to the tight space, we only outline here the approach developed by Foster & Mikhailov and Fedotov. First, it is convenient in (122) to transform the integration over the random field ξ to an integration over the realizations of the field ϕ. ([16, 13]) In this case, the Lagrangian of the statistical weight results:

$$\mathcal{L}[\phi] = \int \mathrm{d}r \left\{ \frac{\partial \phi}{\partial s} + \frac{\delta F}{\delta \phi} \right\}^2, \tag{124}$$

and we obtain

$$P[\phi_{stable}(\boldsymbol{r},t)|\phi_{meta}(\boldsymbol{r},0)] \sim \exp\left\{ -\frac{\mathcal{S}[\phi_{stable}(\boldsymbol{r},t)|\phi_{meta}(\boldsymbol{r},0)]}{2\gamma} \right\}, \tag{125}$$

where

$$\mathcal{S}[\phi] = \inf \int_0^t \mathrm{d}s\, \mathcal{L}[\phi], \tag{126}$$

The action functional $\mathcal{S}[\phi]$, taken along the most probable field realization, satisfies the Hamilton–Jacobi equation:

$$\frac{\partial \mathcal{S}}{\partial \tau} + H = 0, \tag{127}$$

where:

$$H = \int \left\{ \frac{1}{2} (\frac{\delta \mathcal{S}}{\delta \phi})^2 - \frac{\delta \mathcal{S}}{\delta \phi}\, \frac{\delta F}{\delta \phi} \right\} \mathrm{d}r \tag{128}$$

with the initial condition $\mathcal{S}[\phi_{meta}(\boldsymbol{r},0), \phi_{meta}(\boldsymbol{r},0)] = 0$. For functional derivation techniques we refer to ([24]). The Lagrangian $\mathcal{L}[\phi]$ does not contain the time explicitly, so the functional $\mathcal{S}[\phi]$ may be written as:

$$\mathcal{S}[\phi] = W[\phi] - h\, t \tag{129}$$

where h is a constant and $W[\phi]$ satisfies:

$$H(\phi, \frac{\delta W}{\delta \phi}) = h \tag{130}$$

with the condition $W[\phi_{meta}(\boldsymbol{r}), \phi_{meta}(\boldsymbol{r})] = 0$. As is well known, the expected transition time $\langle \tau \rangle$ is the inverse of the transition probability per unit time p_i. To find p_i it is necessary to minimize the action functional in (126) with respect to t. This gives $h = 0$, and we get for p_i

$$p_i \sim \mathrm{e}^{-\frac{1}{2\gamma} W[\phi_{unst}(\boldsymbol{r})|\phi_{meta}(\boldsymbol{r})]} \tag{131}$$

The solution of (126,127) (with $h = 0$) may be written as:

$$W[\phi|\phi_{meta}] = 2\{U[\phi] - U[\phi_{meta}]\} \tag{132}$$

Hence, $\langle\tau\rangle$ results to be

$$\langle\tau\rangle = \tau_0 \, \mathrm{e}^{\frac{1}{\gamma}U[\phi_{unst}(\boldsymbol{r})] - U[\phi_{meta}\boldsymbol{r})]} \tag{133}$$

The factor τ_0 is determined by the curvature of $\boldsymbol{U}[\phi]$ at its extrema and is negligibly short compared with the average time $\langle\tau\rangle$. This result is a generalization of Kramers formula (see Sect.3.4) for extended systems. ([25])

Decay Time for the Ballast System

It is of particular interest in RD systems to study the effect of the fluctuations induced by external noise, because they can produce transitions between the different metastable states. As discussed earlier, the linearly stable states correspond to attractors (minima) of the LF while the unstable ones are saddle points, defining the barrier between attractors.

In order to account for the effect of fluctuations in our model, we need to include in our time–evolution equation (111) a fluctuation term, modelled as an additive noise source, yielding a stochastic partial differential equation for the random field $T(y,t)$:

$$\partial_t T(y,t) = \partial^2_{yy} T - T + T_h \theta(T - T_c) + \xi(y,t). \tag{134}$$

The simplest assumption about the fluctuation term $\xi(y,t)$ is that it is Gaussian white noise with zero mean value and a correlation function given by:

$$\langle \xi(y,t)\, \xi(y',t') \rangle = 2\,\gamma\, \delta(t - t')\, \delta(y - y'), \tag{135}$$

where γ denotes the noise strength. It is also possible to take into account noise sources yielding a multiplicative noise term, but we shall not consider this possibility here.

Now we will exploit the scheme developed in Sect.5.2. The behavior of $\langle\tau\rangle$ as a function of $\phi_c = T_c/T_h$ for a fixed system size is shown in Fig.16. There is a radical change in the behavior when ϕ_c oversteps a threshold value (ϕ_c^*), as indicated before, due to the change in the relative stability between the homogeneous and nonhomogeneous states. The continuous lines in the figure refer to: the decay of the metastable state towards the absolutely stable one for the line indicated with $\Delta F(\phi_s)$ up to the point ϕ_c^*, while the following line indicates the extention of the lines depicting the value of $\langle\tau\rangle$ from the original state, and viceversa for $\Delta F(\phi_0)$.

The results just obtained will be valid as long as the barrier height between the metastable and the stable states (given by the value of the LF at the unstable state) is large enough, assuring that the Kramers' like formula Eq.(133) applies.

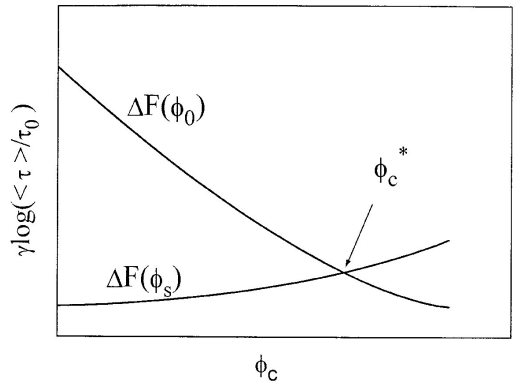

Fig. 16. $\gamma \ln(\langle\tau\rangle/\tau_0)$ vs. ϕ_c for the ballast model with Dirichlet b.c.

5.3 Stochastic Resonance

We present here a brief analysis of this phenomenon in a spatially extended system by exploiting the results obtained using the notion of the *nonequilibrium potential* ([19, 20, 21, 33, 34, 35, 86]) in the ballast resistor model, as this model corresponds (to some approximation) to the continuous limit of the coupled system studied by Lindner *et al.*. The study of the features of the phenomenon of stochastic resonance in the case of extended systems is still incomplete, ([38]) with the particularly interesting recent results of numerical simulations of arrays of coupled nonlinear oscillators ([47, 2, 48]) showing that the coupling enhances the response.

We repeat here the particular form of the (one dimensional) model that we work with

$$\frac{\partial}{\partial t}\phi = D\frac{\partial^2}{\partial x^2}\phi - \phi + \theta(\phi - \phi_c), \tag{136}$$

in the bounded domain $x \in [-L, L]$ and with Dirichlet b.c. at both ends, i.e. $\phi(\pm L, t) = 0$. As discussed earlier, we have the trivial solution $\phi_0(x) = 0$, which is linearly stable and exists for the whole range of parameters, and only one stable nonhomogeneous structure, $\phi_s(x)$, that presents a central excited zone where $\phi_s(x) > \phi_c$. Besides that, we find another similar unstable structure, $\phi_u(x)$, with a smaller central excited zone. This pattern corresponds to the saddle separating both attractors $\phi_0(x)$ and $\phi_s(x)$, see, for instance Fig.14. There are other unstable nonhomogenous solutions, but playing no role in this problem. ([72])

The indicated patterns are extrema of the LF or nonequilibrium potential of our system that reads (see Sect.5.1) ([33, 34, 35, 86])

$$\mathcal{F}[\phi, \phi_c] = \int_{-L}^{+L} \left\{ -\int_0^{\phi} \left(-\phi + \theta[\phi - \phi_c]\right)\, d\phi. + \frac{D}{2}\left(\frac{\partial\phi}{\partial x}\right)^2 \right\} dx. \tag{137}$$

In Fig.14 we show the LF $\mathcal{F}[\phi,\phi_c]$ evaluated at the stationary patterns ϕ_0 ($\mathcal{F}[\phi_0]=0$), $\phi_s(x)$ ($\mathcal{F}^s=\mathcal{F}[\phi_s]$) and $\phi_u(x)$ ($\mathcal{F}^u=\mathcal{F}[\phi_u]$), for a system size $L=1$, as a function of ϕ_c and for two values of D. In the bistable zone, the upper branch of each curve is the LF for $\phi_u(x)$, where $\mathcal{F}$ attains an extremum (as a matter of fact it is a saddle of the nonequilibrium potential). On the lower branch, for $\phi_s(x)$, and also for $\phi_0(x)$, the LF has local minima. For each value of D the curves exist up to a certain critical value of ϕ_c at which both branches collapse. It is interesting to note that, since the LF for $\phi_u(x)$ is always positive and, for $\phi_s(x)$, $\mathcal{F}^s$ is positive for some values of ϕ_c and also $\mathcal{F}^s\to-\infty$ as $\phi_c\to 0$, $\mathcal{F}^s$ vanishes for an intermediate value of $\phi_c=\phi_c^*$, where $\phi_s(x)$ and $\phi_0(x)$ exchange their relative stability.

In order to account for the effect of fluctuations, we include in the time–evolution equation of our model (111) a fluctuation term $\xi(x,t)$, as was discussed in Sect.5.2. We denote the noise strength with γ. According to the scheme discussed in Sect.5.2, we have the Kramers' like result for the first-passage-time $\langle\tau\rangle$ indicated in (133) that we repeat here

$$\langle\tau\rangle=\tau_0\,\exp\left\{\frac{\Delta\mathcal{F}[\phi,\phi_c]}{\gamma}\right\}, \tag{138}$$

where $\Delta\mathcal{F}[\phi,\phi_c]=\mathcal{F}[\phi_{unst}(y),\phi_c]-\mathcal{F}[\phi_{meta}(y),\phi_c]$. The prefactor τ_0 is determined by the curvature of $\mathcal{F}[\phi,\phi_c]$ at its extrema. In the Fig.16 we have shown the form of $\Delta\mathcal{F}[\phi_0,\phi_c]$ (line (b)) and $\Delta\mathcal{F}[\phi_s,\phi_c]$ (line(a)), as a function of ϕ_c. It also corresponds to the behavior of $\ln(\langle\tau\rangle/\tau_0)$.

We now assume that, due to an external harmonic variation, the parameter ϕ_c has an oscillatory part $\phi_c(t)=\phi_c^*+\delta\phi_c\cos(\Omega t+\varphi)$. For the spatially extended problem, we need to evaluate the space–time correlation function $\langle\phi(y,t)\phi(y',t')\rangle$. To do this we will use a simplified point of view, based on the two state approach of MNW, ([50]) that allows us to apply almost directly most of their results. To proceed with the calculation of the correlation function we need to evaluate the transition probabilities between our two states ϕ_0 and ϕ_s,

$$W_\pm=\tau_0^{-1}\exp\left(-\Delta\mathcal{F}[\phi,\phi_c]/\gamma\right), \tag{139}$$

where

$$\Delta\mathcal{F}[\phi,\phi_c]\approx\Delta\mathcal{F}[\phi,\phi_c^*]+\delta\phi_c[\frac{\partial\Delta\mathcal{F}[\phi,\phi_c]}{\partial\phi_c}]_{\phi_c^*}\cos(\Omega t+\varphi).$$

This yields for the transition probabilities

$$W_\pm\approx\frac{1}{2}\Big(\alpha_0\mp\alpha_1\frac{\delta\phi_c}{\gamma}\cos(\Omega t+\varphi)\Big), \tag{140}$$

with

$$\begin{aligned}\alpha_0&\approx\exp(-\Delta\mathcal{F}[\phi,\phi_c^*]/\gamma)\\ \alpha_1&\approx\alpha_0\frac{d\Delta\mathcal{F}}{d\phi_c}|_{\phi_c^*}.\end{aligned} \tag{141}$$

With this identification, and using the fact that $\phi_0 = 0$, only one term remains. Hence, after averaging over the random phase φ, we end up with an expression similar to their correlation function but in which the position of their minima, $\pm c$, is replaced by $c^2 = \phi_u(x)^2$.

To obtain the generalized susceptibility $S(\kappa, \omega)$, we need to perform the Fourier transform of the correlation function in time as well as in space. Due to the fact that the space and time dependence of the correlation function factorize, $S(\kappa, \omega)$ factorizes too, and it is enough to analyze its time dependence. The Fourier transform of this time dependence yields a function analogous to the usual power spectrum function $S(\omega)$. ([50]) Finally, the result for the SNR is

$$\text{SNR} \sim (\Lambda\lambda\gamma^{-1})^2 \exp\Big(-2\Delta\mathcal{F}[\phi, \phi_c^*]/\gamma\Big), \tag{142}$$

where λ is an estimation of the potential curvature at the potential minima (as given by the linear stability eigenvalue), and

$$\Lambda \sim \frac{d\Delta\mathcal{F}}{d\phi_c}|_{\phi_c^*}\delta\phi_c. \tag{143}$$

Equation (142) is analogous to what has been obtained in zero dimensional systems, but $\Delta\mathcal{F}[\phi, \phi_c^*]$ contains all the information regarding the spatially extended character of the system.

In Fig.17 we show the dependence of the present result for the SNR on γ, for typical values of the parameters (same as in Fig.16), and different values of D. It is seen that the response increases for increasing values of D. Also in Fig.16 we show the dependence of the maximum of the SNR as a function of D (that plays here the role of the coupling parameter). These results are in good qualitative agreement with recent numerical results for a system of coupled nonlinear oscillators. ([47, 2, 48, 84])

It is worth remarking here that the present calculation breaks down for large values of D. This is due to the fact that, for increasing D, the curves in Fig.14 shift to the left while the barrier separating the attractors tends to zero. It is also worth noting that, except for the approximation involved in the Kramers' like expression in (138) and the two level approximation used for the evaluation of the correlation function, all the previous results (form of the patterns, nonequilibrium potential) are analytically exact. However, in a more careful analysis of the problem, as indicated by the present rough calculation, it seems reasonable to expect different strengths for the SR phenomena for different wave lengths, as the dependence of the generalized susceptibility $S(\kappa, \omega)$ on κ and ω –that will not necessarily factorize– also imply that SNR $\sim$ SNR(κ, ω).

6 Conclusions

In this set of lectures we have presented some elements of dynamical systems, stochastic processes and reaction-diffusion models, in order to build

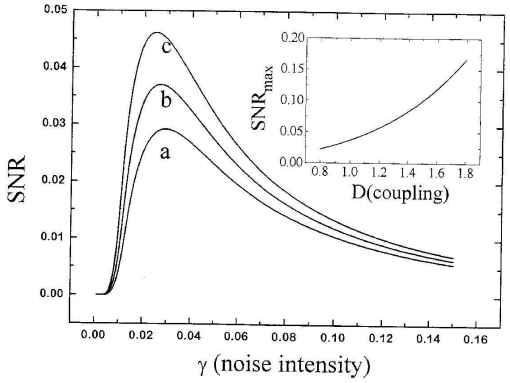

Fig. 17. SNR as a function of the noise intensity γ (Eq.(17)), for (a) $D = 0.9$, (b) $= 1.0$, (c) $= 1.1$. We fixed $\phi_c = \phi_c^*$, $L = 1$, $\delta\phi_c = 0.01$ and $\Omega = 0.01$. The insert shows the maximum of SNR as a function of D.

the necessary background to face the problem of exploiting the notion of the nonequilibrium potential in extended systems. Through the knowledge of such nonequilibrium potential we have studied some simple (piecewise linear) reaction–diffusion models representing bistable systems.

Such nonequilibrium potentials have enabled us to analyze the global stability of the system and the change in the relative stability between attractors as some parameter (threshold parameter, albedo o partial reflectivity at the borders, and/or the system length) is varied. Through this Lyapunov functional, we have also computed the mean lifetime or mean first-passage time for the decay of the metastable stationary state. In this way, we have shown how some parameters or b.c. not only rule the relative stability between attractors, but also the response of the system under the effect of fluctuations.

As a novel aspect we have discussed how to exploit the previous results in order to be able to study the phenomenon of stochastic resonance in extended systems. Such studies are scarce due to the almost unsurmountable difficulties they present. ([38, 83, 49, 84])

We are fairly certain that the present form of analysis could be extended to the general activator–inhibitor system and other multicomponent systems. There is strong evidence of the possibilities of obtaining the nonequilibrium potential for more general situations as shown in some recent papers. ([9, 10, 36]) The possible applications in chemical and biological systems, ([56, 3, 6, 80]) and their relation with spatio–temporal synchronization problems, ([44]) are very well known.

Acknowledgements

The author thanks R. Graham, D.H. Zanette, R. Deza, E. Tirapegui, R. Toral, G. Izús, M. Kuperman, G. Drazer, F.Castelpoggi for discussions and/or

collaborations, V. Grunfeld for a critical reading of the manuscript and A. Sánchez, M. Kuperman and F.Castelpoggi for their help with the figures. Partial support from CONICET, Argentina, and from Fundación Antorchas, are also acknowledged.

References

1. Bulsara A.R., Chilleni S., Kiss L., McClintock P.V.E., Mannella R., Marchesoni F.V., Nicolis G., Wiesenfeld K., editors (1995): *Proc. 2nd. Int. Workshop on Fluctuations in Physics and Biology: Stochastic Resonance, Signal Processing and Related Phenomena*, Il Nuovo Cim. **D 17**.
2. Bulsara A., Gammaitoni L. (1996): Physics Today **49**, 39.
3. Bezrukov S.M., Vodyanoy I. (1995): Nature **378**, 362.
4. Brink D.M., (1980): Prog. Part. & Nucl. Phys. **4**, 323.
5. Castelpoggi F., Wio H.S., Zanette D.H. (1996): Int. J. Mod. Phys. B (in press).
6. Collins J.J., Chow C.C., Imhoff T.T. (1995): Nature **376**, 236.
7. Cross P.C. (1988): *Theoretical Methods in Pattern Formation in Physics, Chemistry and Biology*, in *Far From Equilibrium Phase Transitions*, Ed.L.Garrido (Springer-Verlag, Berlin).
8. Cross P.C., Hohenberg P. (1993): Rev.Mod.Phys. **65**, 851.
9. Descalzi O., Graham R. (1992): Phys. Lett. A **170**, 84.
10. Descalzi O., Graham R. (1994): Z.Phys.B **93**, 509.
11. Doering C.R. (1991): *Modelling Complex Systems: Stochastic Processes, Stochastic Differential Equations and Fokker-Planck Equations*, in *Lectures in Complex Systems*, **vol.III**, Ed.L.Nadel and D.Stein, (Addison-Wesley, N.Y.).
12. Drazer G., Wio H.S. (1996): *Nonequilibrium potential for an activator–inhibitor model with fast inhibition*, submited to Physica A.
13. Fedotov S.P. (1993): Phys. Lett. A **176**, 220.
14. Fife P.C. (1978): *Mathematical Aspects of Reacting and Diffusing Systems*, (Springer-Verlag, Berlin).
15. Fife P.C. (1984): *Current Topics in Reaction-Diffusion Systems*, in *Nonequilibrium Cooperative Phenomena in Physics and Related Fields*, Ed.M.G.Velarde (Plenum, N.Y.).
16. Foster A., Mikhailov A.S. (1988): Phys. Lett. A **126**, 459.
17. Gardiner C.W. (1985): *Handbook of Stochastic Methods*, 2nd Ed. (Springer-Verlag, Berlin).
18. Goldstein R.E., Muraki D.J., Petrich D.M. (1996): Phys. Rev. E., to appear.
19. Graham R. (1978): in *Lecture Notes in Physics*, vol. 84 (Springer–Verlag, Berlin).
20. Graham R. (1987): *Weak Noise Limit and Nonequilibrium Potentials of Dissipative Dynamical Systems*, in *Instabilities and Nonequilibrium Structures*, Eds.E.Tirapegui and D.Villaroel (D.Reidel, Dordrecht).
21. Graham R., Tel T. (1990): Phys. Rev. A **42**, 4661.
22. Gunton J.D., Droz M. (1983): *Introduction to the theory of metastable and unstable states*. Lecture notes in physics vol 183, (Springer-Verlag, Berlin).
23. Haken H. (1978): *Synergetics: An Introduction*, 2nd Ed. (Springer-Verlag, N.Y.).

24. Hänggi P. (1985): *The Functional Derivative and its use in the Description of Noisy Dynamical Systems*, in *Stochastic Processes Applied to Physics*, Eds. L.Pesquera and M.A.Rodriguez (World Scientific, Singapore).
25. Hängi P., Talkner P., Borkovec M. (1990): Rev. Mod. Phys, **62**, 251.
26. Hassan S.A., Kuperman M.N., Wio H.S., Zanette D.H. (1994): Physica A **206**, 380.
27. Hassan S.A., Zanette D.H., Wio H.S. (1994): J.Phys. A **27**, 5129.
28. Hassan S.A., Zanette D.H. (1995): Physica A **214**, 435.
29. Hernandez-García E., Viñals J.R., Toral R., San Miguel M. (1993): Phys. Rev. Lett. **70**, 3573.
30. Hohenberg P.C., Halperin B.I. (1977): Rev. Mod. Phys. **49**, 535.
31. Horsthemke W., Lefever R. (1984): *Noise-Induced Transitions*, (Springer-Verlag, Berlin).
32. Inchiosa M.E., Bulsara A. (1996): Phys. Rev. E **53**, R2021.
33. Izús G., Deza R., Ramírez O., Wio H.S., Zanette D.H., Borzi C. (1995): Phys. Rev. E **52**, 129.
34. Izús G., Wio H.S., Reyes de Rueda J., Ramírez O., Deza R. (1996): Int. J. Mod. Phys. B **10**, 1273.
35. Izús G., Wio H.S., Zanette D.H., Deza R., Von Haeften B. (1996): *Evolution of bistable reaction-diffusion systems within a Lyapunov functional framework*, submitted to Physica A.
36. Izús G., Deza R., Wio H.S., Borzi C. (1996): Phys. Rev. E, (in press).
37. Jüng P. (1993): Phys. Reports **234**, 175.
38. Jüng P., Mayer-Kress G. (1995): Phys. Rev. Lett. **74**, 208.
39. Keizer J. (1987): *Statistical Thermodynamics of Nonequilibrium Processes*, (Springer-Verlag, Berlin).
40. Kerszberg M. (1983): Phys. Rev. A **28**, 1198.
41. Kirkady J.S. (1992): Rep.Prog.Phys. **55**, 723.
42. Koga S., Kuramoto Y. (1980): Prog.Theor.Phys. **63**, 106.
43. Kreuzer H.J. (1984): *Nonequilibrium Thermodynamics and its Statistical Foundations*, (Clarendon P., Oxford).
44. Kuramoto Y. (1984): *Chemical Oscillations, Waves, Turbulence*, (Springer-Verlag, Berlin).
45. Langer J.S. (1987): *Lectures in the Theory of Pattern Formation*, in *Chance and Matter*, Eds. Souletie J., Vannimenus J., Stora R. (North-Holland, Amsterdam).
46. Langouche F., Roekaerts D., Tirapegui E.(1982): *Functional Integration and Semiclassical Expansions* (D.Reidel Pub.Co., Dordrecht).
47. Lindner J.F., Meadows B.K., Ditto W.L., Inchiosa M.E., Bulsara A. (1995): Phys. Rev. Lett. **75**, 3.
48. Lindner J.F., Meadows B.K., Ditto B.K., Inchiosa M.E., Bulsara A. (1996): Phys. Rev. E **53**, 2081.
49. Marchesoni F., Gammaitoni L., Bulsara A.R. (1996): Phys. Rev. Lett. **76**, 2609.
50. McNamara B., Wiesenfeld K. (1989): Phys. Rev. A **39**, 4854.
51. Malchow H., Schimansky-Geier L. (1985): *Noise and Diffusion in Bistable Nonequilibrium Systems*, (Teubner, Berlin).
52. Meinhardt H. (1992): Rep.Prog.Phys. **55**, 797.
53. Mikhailov A.S. (1990): *Foundations of Synergetics I*, (Springer-Verlag, Berlin).

54. Mikhailov A.S., Loskutov A.Yu. (1992): *Foundations of Synergetics II*, (Springer- Verlag, Berlin).
55. Montagne R., Hernández-Garcia E., San Miguel M. (1996): Physica D, **96**, 47.
56. Moss F. (1992): in *Some Problems in Statistical Physics*, edited by G. Weiss (SIAM, Philadelphia).
57. Moss F., Bulsara A., Shlesinger M., editors (1993): *Proceedings of the NATO Advanced Research Workshop on Stochastic Resonance in Physics and Biology*, J. Stat. Phys. **70** No. 1/2.
58. Murray J.D. (1989): *Mathematical Biology* (Springer-Verlag, Berlin).
59. Newell A.C. (1989): *The Dynamics and Analysis of Patterns*, in *Complex Systems*, Ed.D.Stein, (Addison-Wesley, N.Y.).
60. Nicolis G. (1986): Rep.Prog.Phys. *49*, 873.
61. Nicolis G. (1989): *Physics of Far-from-Equilibrium Systems and Self-Organization*, in *The New Physics*, Ed.P.Davis, (Cambridge U.P., Cambridge).
62. Nicolis G. (1995): *Introduction to Nonlinear Science*, (Cambridge U.P., Cambridge).
63. Nicolis G., Prigogine I. (1977): *Self-Organization in Nonequilibrium Systems*, (Wiley, N.Y.)
64. Ohta T. (1989): Prog.Theor.Phys. **99**, 33.
65. Ohta T., Mimura M., Kobayashi K. (1989): Physica D **34**, 115.
66. Ohta T., Ito A., Tetsuka A. (1990): Phys. Rev. A **42**, 3225.
67. Petrich D.M., Goldstein R.E. (1994): Phys. Rev. Lett. **72**, 1120.
68. Prigogine I. (1980): *From Being to Becoming* (W.H.Freeman, San Francisco).
69. Reichl L.E. (1980): *A Modern Course in Statistical Physics*, (Univ.Texas Press. Austin).
70. Risken H. (1983): *The Fokker-Planck Equation*, (Springer-Verlag, Berlin).
71. San Miguel M. (1985): *Stochastic Methods and Models in the Dynamics of Phase Transitions*, in *Stochastic Processes Applied to Physics*, Eds. L.Pesquera and M.A.Rodriguez (World Scientific, Singapore).
72. Schat C.L., Wio H.S. (1992): Physica A **180**, 295.
73. Schulman L.S. (1981): *Techniques and Applications of Path Integration* (Wiley, New York).
74. Skocpol W.J., Beasley M.R., Tinkham M. (1974): J. Appl. Phys. **45**, 4054.
75. de la Torre M., Rehberg I. (1990): Phys. Rev. A **42**, 2096 and 5998.
76. van Kampen N. (1982): *Stochastic Processes in Physics and Chemistry*, (North Holland).
77. Viñals J., Hernandez-García E., San Miguel M., Toral R. (1991): Phys. Rev. A **44**, 1123.
78. Walgraef D. (1988): *Structures Spatiales loin de l'equilibre*, (Mason, Paris).
79. Weidenmüller H.A., (1980): Prog. Part. & Nucl. Phys. **4**, 123.
80. Wiesenfeld K., Moss F. (1995): Nature **373**, 33.
81. Wio H.S. (1990): *Introducción a las Integrales de Camino* (Univ.Illes Balears, Palma de Mallorca, Spain).
82. Wio H.S. (1994): *An Introduction to Stochastic Processes and Nonequilibrium Statistical Physics*, (World Scientific, Singapore).
83. Wio H.S. (1996): Phys. Rev. E **54**, R3075.
84. Wio H.S., Castelpoggi F. (1996): *Stochastic Resonance in a Reaction-Diffusion System: Enhancement due to Coupling*, Proc.Conf.UPoN'96, Szeged, September 1996, C.R. Doering, L.B. Kiss and M. Shlesinger Editors (World Scientific, Singapore).

85. Wio H.S, Izús G., Deza R., Ramírez O., Borzi C. (1993): J.Phys.A: Math.Gen. **26**, 4281.
86. Zanette D.H., Wio H.S., Deza R. (1996): Phys. Rev. E **53**, 353.